

623.172  
NATIONAL ADVISORY COMMITTEE  
FOR AERONAUTICS  
FEB 5 1922  
MAILED

AERO. & ASTRO. LIBRARY

MASS. INST. TECH.  
FEB 10 1923  
LIBRARY

TO: *Library, M. J. J.*

NATIONAL ADVISORY COMMITTEE  
FOR AERONAUTICS

REPORT No. 156

*c.3*

THE ALTITUDE EFFECT ON AIR SPEED INDICATORS—II

By H. N. EATON and W. A. MacNAIR



WASHINGTON  
GOVERNMENT PRINTING OFFICE  
1922



---

---

**REPORT No. 156**

---

**THE ALTITUDE EFFECT ON AIR SPEED INDICATORS—II**

IN TWO PARTS

**CONTINUATION OF REPORT No. 110**

**By H. N. EATON and W. A. MacNAIR**  
**Bureau of Standards**

REPORT No. 158

THE ALTITUDE EFFECT ON AIR SPEED INDICATORS - II

CONTINUATION OF REPORT No. 110

By H. N. EATON and W. A. MacAIR  
Bureau of Standards



## INDEX.

### PART I. EXPERIMENTS WITH VENTURI TUBES.

	Page.
1. Introduction.....	7
2. Theory of the performance of air speed pressure nozzles.....	7
3. Theory of the calibration of air speed indicators.....	9
4. Theory of the altitude correction.....	10
5. Nozzles tested in this investigation.....	11
6. Standard air density.....	12
7. Determination of constants of the nozzles.....	12
8. Determination of the form of $\theta \left( \frac{\rho_0}{\rho}, \frac{Dv_i\rho}{\mu} \right)$ .....	20
Description of low-pressure wind tunnel.....	20
Low-pressure wind-tunnel tests.....	24
9. Performance of Venturi nozzles at very high speeds.....	29
10. Discussion of data.....	30

### PART II. THE ALTITUDE CORRECTION.

1. Introduction.....	37
2. The compressibility correction for Pitot nozzles.....	37
3. The compressibility correction for Venturi nozzles.....	37
4. The density correction for Pitot nozzles.....	38
5. The density correction for Venturi nozzles.....	38
6. The viscosity correction for Venturi nozzles.....	38
7. Illustrative examples.....	42
8. Conclusions.....	44

### NOTATION.

- $p$ =pressure delivered by Pitot nozzle.  
 $p_1$ =differential pressure delivered by Venturi or Pitot-Venturi nozzle.  
 $s$ =suction delivered by Venturi tube as distinguished from differential pressure delivered by Pitot-Venturi tube.  
 $h$ =head of water corresponding to  $p$ .  
 $h_1$ =head of water corresponding to  $p_1$ .  
 $K$ =constant of Pitot tube.  
 $K_1$ =constant of Venturi tube.  
 $d$ =density of water in manometers ( $d=1$  throughout this report).  
 $v$ =true air speed.  
 $v_i$ =indicated air speed.  
 $t$ =air temperature in degrees centigrade.  
 $T$ =air temperature in degrees centigrade absolute.  
 $B$ =barometric pressure.  
 $\rho$ =air density.  
 $\mu$ =air viscosity.  
 $E$ =compressibility modulus of elasticity (adiabatic).  
 $\kappa$ =specific heat ratio for air.  
 $r$ =relative density= $\frac{\rho}{\rho_0}$ .  
 $g$ =acceleration of gravity.  
 $e$ =base of natural logarithms.  
 $D$ =a linear dimension.  
 $C$ =a constant.  
 $Z = \frac{Dv_i\rho}{\mu}$ .

$F, \phi, \theta, \psi$ =functional symbols.

Subscript zero refers to standard conditions.



INDEX

Part I. Elementary Wave Theory of Light

1. The propagation of light in a homogeneous medium . . . . . 1

2. The propagation of light in an anisotropic medium . . . . . 15

3. The propagation of light in a dispersive medium . . . . . 35

4. The propagation of light in a medium with a periodic structure . . . . . 55

5. The propagation of light in a medium with a random structure . . . . . 75

6. The propagation of light in a medium with a periodic structure and a random structure . . . . . 95

7. The propagation of light in a medium with a periodic structure and a random structure, and a dispersive medium . . . . . 115

8. The propagation of light in a medium with a periodic structure and a random structure, and a dispersive medium, and an anisotropic medium . . . . . 135

Part II. The Theory of Diffraction

1. The theory of diffraction by a plane surface . . . . . 155

2. The theory of diffraction by a plane surface, and a dispersive medium . . . . . 175

3. The theory of diffraction by a plane surface, and a dispersive medium, and an anisotropic medium . . . . . 195

4. The theory of diffraction by a plane surface, and a dispersive medium, and an anisotropic medium, and a periodic structure . . . . . 215

5. The theory of diffraction by a plane surface, and a dispersive medium, and an anisotropic medium, and a periodic structure, and a random structure . . . . . 235

NOTATION

$\mathbf{r}$  position vector of point  $P$  . . . . .

$\mathbf{r}_0$  position vector of point  $P_0$  . . . . .

$\mathbf{r}_1$  position vector of point  $P_1$  . . . . .

$\mathbf{r}_2$  position vector of point  $P_2$  . . . . .

$\mathbf{r}_3$  position vector of point  $P_3$  . . . . .

$\mathbf{r}_4$  position vector of point  $P_4$  . . . . .

$\mathbf{r}_5$  position vector of point  $P_5$  . . . . .

$\mathbf{r}_6$  position vector of point  $P_6$  . . . . .

$\mathbf{r}_7$  position vector of point  $P_7$  . . . . .

$\mathbf{r}_8$  position vector of point  $P_8$  . . . . .

$\mathbf{r}_9$  position vector of point  $P_9$  . . . . .

$\mathbf{r}_{10}$  position vector of point  $P_{10}$  . . . . .

$\mathbf{r}_{11}$  position vector of point  $P_{11}$  . . . . .

$\mathbf{r}_{12}$  position vector of point  $P_{12}$  . . . . .

$\mathbf{r}_{13}$  position vector of point  $P_{13}$  . . . . .

$\mathbf{r}_{14}$  position vector of point  $P_{14}$  . . . . .

$\mathbf{r}_{15}$  position vector of point  $P_{15}$  . . . . .

$\mathbf{r}_{16}$  position vector of point  $P_{16}$  . . . . .

$\mathbf{r}_{17}$  position vector of point  $P_{17}$  . . . . .

$\mathbf{r}_{18}$  position vector of point  $P_{18}$  . . . . .

$\mathbf{r}_{19}$  position vector of point  $P_{19}$  . . . . .

$\mathbf{r}_{20}$  position vector of point  $P_{20}$  . . . . .

$\mathbf{r}_{21}$  position vector of point  $P_{21}$  . . . . .

$\mathbf{r}_{22}$  position vector of point  $P_{22}$  . . . . .

$\mathbf{r}_{23}$  position vector of point  $P_{23}$  . . . . .

$\mathbf{r}_{24}$  position vector of point  $P_{24}$  . . . . .

$\mathbf{r}_{25}$  position vector of point  $P_{25}$  . . . . .

$\mathbf{r}_{26}$  position vector of point  $P_{26}$  . . . . .

$\mathbf{r}_{27}$  position vector of point  $P_{27}$  . . . . .

$\mathbf{r}_{28}$  position vector of point  $P_{28}$  . . . . .

$\mathbf{r}_{29}$  position vector of point  $P_{29}$  . . . . .

$\mathbf{r}_{30}$  position vector of point  $P_{30}$  . . . . .

$\mathbf{r}_{31}$  position vector of point  $P_{31}$  . . . . .

$\mathbf{r}_{32}$  position vector of point  $P_{32}$  . . . . .

$\mathbf{r}_{33}$  position vector of point  $P_{33}$  . . . . .

$\mathbf{r}_{34}$  position vector of point  $P_{34}$  . . . . .

$\mathbf{r}_{35}$  position vector of point  $P_{35}$  . . . . .

$\mathbf{r}_{36}$  position vector of point  $P_{36}$  . . . . .

$\mathbf{r}_{37}$  position vector of point  $P_{37}$  . . . . .

$\mathbf{r}_{38}$  position vector of point  $P_{38}$  . . . . .

$\mathbf{r}_{39}$  position vector of point  $P_{39}$  . . . . .

$\mathbf{r}_{40}$  position vector of point  $P_{40}$  . . . . .

$\mathbf{r}_{41}$  position vector of point  $P_{41}$  . . . . .

$\mathbf{r}_{42}$  position vector of point  $P_{42}$  . . . . .

$\mathbf{r}_{43}$  position vector of point  $P_{43}$  . . . . .

$\mathbf{r}_{44}$  position vector of point  $P_{44}$  . . . . .

$\mathbf{r}_{45}$  position vector of point  $P_{45}$  . . . . .

$\mathbf{r}_{46}$  position vector of point  $P_{46}$  . . . . .

$\mathbf{r}_{47}$  position vector of point  $P_{47}$  . . . . .

$\mathbf{r}_{48}$  position vector of point  $P_{48}$  . . . . .

$\mathbf{r}_{49}$  position vector of point  $P_{49}$  . . . . .

$\mathbf{r}_{50}$  position vector of point  $P_{50}$  . . . . .

$\mathbf{r}_{51}$  position vector of point  $P_{51}$  . . . . .

$\mathbf{r}_{52}$  position vector of point  $P_{52}$  . . . . .

$\mathbf{r}_{53}$  position vector of point  $P_{53}$  . . . . .

$\mathbf{r}_{54}$  position vector of point  $P_{54}$  . . . . .

$\mathbf{r}_{55}$  position vector of point  $P_{55}$  . . . . .

$\mathbf{r}_{56}$  position vector of point  $P_{56}$  . . . . .

$\mathbf{r}_{57}$  position vector of point  $P_{57}$  . . . . .

$\mathbf{r}_{58}$  position vector of point  $P_{58}$  . . . . .

$\mathbf{r}_{59}$  position vector of point  $P_{59}$  . . . . .

$\mathbf{r}_{60}$  position vector of point  $P_{60}$  . . . . .

$\mathbf{r}_{61}$  position vector of point  $P_{61}$  . . . . .

$\mathbf{r}_{62}$  position vector of point  $P_{62}$  . . . . .

$\mathbf{r}_{63}$  position vector of point  $P_{63}$  . . . . .

$\mathbf{r}_{64}$  position vector of point  $P_{64}$  . . . . .

$\mathbf{r}_{65}$  position vector of point  $P_{65}$  . . . . .

$\mathbf{r}_{66}$  position vector of point  $P_{66}$  . . . . .

$\mathbf{r}_{67}$  position vector of point  $P_{67}$  . . . . .

$\mathbf{r}_{68}$  position vector of point  $P_{68}$  . . . . .

$\mathbf{r}_{69}$  position vector of point  $P_{69}$  . . . . .

$\mathbf{r}_{70}$  position vector of point  $P_{70}$  . . . . .

$\mathbf{r}_{71}$  position vector of point  $P_{71}$  . . . . .

$\mathbf{r}_{72}$  position vector of point  $P_{72}$  . . . . .

$\mathbf{r}_{73}$  position vector of point  $P_{73}$  . . . . .

$\mathbf{r}_{74}$  position vector of point  $P_{74}$  . . . . .

$\mathbf{r}_{75}$  position vector of point  $P_{75}$  . . . . .

$\mathbf{r}_{76}$  position vector of point  $P_{76}$  . . . . .

$\mathbf{r}_{77}$  position vector of point  $P_{77}$  . . . . .

$\mathbf{r}_{78}$  position vector of point  $P_{78}$  . . . . .

$\mathbf{r}_{79}$  position vector of point  $P_{79}$  . . . . .

$\mathbf{r}_{80}$  position vector of point  $P_{80}$  . . . . .

$\mathbf{r}_{81}$  position vector of point  $P_{81}$  . . . . .

$\mathbf{r}_{82}$  position vector of point  $P_{82}$  . . . . .

$\mathbf{r}_{83}$  position vector of point  $P_{83}$  . . . . .

$\mathbf{r}_{84}$  position vector of point  $P_{84}$  . . . . .

$\mathbf{r}_{85}$  position vector of point  $P_{85}$  . . . . .

$\mathbf{r}_{86}$  position vector of point  $P_{86}$  . . . . .

$\mathbf{r}_{87}$  position vector of point  $P_{87}$  . . . . .

$\mathbf{r}_{88}$  position vector of point  $P_{88}$  . . . . .

$\mathbf{r}_{89}$  position vector of point  $P_{89}$  . . . . .

$\mathbf{r}_{90}$  position vector of point  $P_{90}$  . . . . .

$\mathbf{r}_{91}$  position vector of point  $P_{91}$  . . . . .

$\mathbf{r}_{92}$  position vector of point  $P_{92}$  . . . . .

$\mathbf{r}_{93}$  position vector of point  $P_{93}$  . . . . .

$\mathbf{r}_{94}$  position vector of point  $P_{94}$  . . . . .

$\mathbf{r}_{95}$  position vector of point  $P_{95}$  . . . . .

$\mathbf{r}_{96}$  position vector of point  $P_{96}$  . . . . .

$\mathbf{r}_{97}$  position vector of point  $P_{97}$  . . . . .

$\mathbf{r}_{98}$  position vector of point  $P_{98}$  . . . . .

$\mathbf{r}_{99}$  position vector of point  $P_{99}$  . . . . .

$\mathbf{r}_{100}$  position vector of point  $P_{100}$  . . . . .



## REPORT No. 156.

### THE ALTITUDE EFFECT ON AIR-SPEED INDICATORS—II.

CONTINUATION OF REPORT NO. 110.

By H. N. EATON and W. A. MACNAIR.

#### SUMMARY.

This report is the second part of an investigation on the altitude effect on air-speed indicators, conducted by the Aeronautic Instruments Section of the Bureau of Standards under research authorization formulated and recommended by the subcommittee on aerodynamics and approved by the National Advisory Committee for Aeronautics.

It has hitherto been assumed that the correction of the readings of differential pressure type air-speed indicators to true air speed could be accomplished with sufficient accuracy by the use of a multiplying factor depending on the square root of the air density. It has been recognized that the compressibility of the air introduced an error into the air-speed reading, but this effect has been assumed to be negligible over the range of speeds commonly attained.

Only quite recently has it been shown that a third physical property of the atmosphere, its viscosity, affects appreciably the readings of Venturi and Pitot-Venturi indicators at low speeds and at high altitudes. In an investigation described in Report No. 110 of the National Advisory Committee for Aeronautics, "The Altitude Effect on Air Speed Indicators," by M. D. Hersey, F. L. Hunt, and H. N. Eaton, it was shown that under certain conditions, particularly for the relatively low-speed flight of dirigible airships, the viscosity effect was important; but the data obtained were not sufficiently accurate to allow a determination of the general law to be made.

The present report describes a more recent investigation, in which the data obtained were sufficiently accurate and complete to enable the viscosity correction to be deduced quantitatively for a number of the air-speed pressure nozzles in common use.

The report opens with a discussion of the theory of the performance of air-speed nozzles and of the calibration of the indicators, from which the theory of the altitude correction is developed. Then follows the determination of the performance characteristics of the nozzles and the calibration constants used for the indicators. In the latter half of the report, the viscosity correction is computed for the Zahm Pitot-Venturi nozzles, Army and Navy types, which are the most commonly used air-speed nozzles in the United States. It will be found that the viscosity correction is far from negligible, since under certain conditions it may amount to 20 per cent or more of the indicated air speed. Tables and plots are given to enable the readings of Pitot type and Zahm Pitot-Venturi type indicators to be corrected for any atmospheric conditions which may be experienced by either heavier-than-air or lighter-than-air craft and for air speeds up to approximately 200 miles per hour. Evidence is also adduced tending to show that the effect of the compressibility of the atmosphere on the performance of Venturi air-speed nozzles is not numerically greater than the corresponding effect on Pitot tubes, and can be neglected over the range of flying speeds commonly attained to-day.



REPORT No. 152

THE ALTITUDE EFFECT ON AIR SPEED INDICATORS

W. G. WATSON  
A. G. WATSON

ABSTRACT

The present investigation was conducted to determine the effect of altitude on the accuracy of air speed indicators. The results show that the accuracy of these instruments is affected by the change in air density with altitude. The error is greatest at high altitudes and is proportional to the square of the altitude. The results are presented in a series of graphs and tables.

The investigation was conducted at the Naval Air Station, San Diego, California. The altitudes used were 0, 1000, 2000, 3000, 4000, 5000, 6000, 7000, 8000, 9000, and 10000 feet. The air speed indicators used were of the pitot-static type. The results show that the accuracy of these instruments is affected by the change in air density with altitude. The error is greatest at high altitudes and is proportional to the square of the altitude. The results are presented in a series of graphs and tables.

The results of the investigation show that the accuracy of air speed indicators is affected by the change in air density with altitude. The error is greatest at high altitudes and is proportional to the square of the altitude. The results are presented in a series of graphs and tables. The graphs show that the error increases with altitude and is proportional to the square of the altitude. The tables show the same results in tabular form.

The results of the investigation show that the accuracy of air speed indicators is affected by the change in air density with altitude. The error is greatest at high altitudes and is proportional to the square of the altitude. The results are presented in a series of graphs and tables.



## REPORT No. 156.

### THE ALTITUDE EFFECT ON AIR-SPEED INDICATORS—II.

---

#### PART I.

#### EXPERIMENTS WITH VENTURI TUBES.

---

##### 1. INTRODUCTION.

The air-speed indicators commonly used in aeronautics may be classified as follows:<sup>1</sup>

1. Rotating surface instruments.
2. Direct impact instruments.
3. Differential pressure instruments.

Of these three classes, the third is by far the most generally used. This class of air-speed indicators may be subdivided as follows:

- (a) Pitot type.
- (b) Venturi type.
- (c) Pitot-Venturi type.

This paper is concerned only with the differential pressure type of air-speed indicator, and, in particular, with Venturi and Pitot-Venturi instruments, since the method of correcting the readings of Pitot indicators is well known.

A clear understanding of the altitude correction for differential pressure type air-speed indicators requires recognition at the outset of the fact that such instruments consist of two distinct parts: (1) An air-speed pressure nozzle of one of the types mentioned, in which the motion of the air stream relative to the nozzle produces a differential pressure; and (2) a pressure gauge by means of which this differential pressure is measured. The dial of this gauge is graduated in terms of air speed instead of pressure.

It is clear, therefore, that two relations are involved in the corrections of the air-speed readings to true air speed:

- (a) The relation between the actual air speed and the corresponding differential pressure produced by the nozzle.
- (b) The relation between the differential pressure produced by the nozzle and the reading of the indicator.

These will be discussed in turn.

##### 2. THEORY OF THE PERFORMANCE OF AIR-SPEED PRESSURE NOZZLES.

The differential pressure developed by any air-speed pressure nozzle may conceivably depend on the shape of the nozzle, on its absolute size, on its speed relative to the medium in which it is placed, and on the density, viscosity, and compressibility of the medium.<sup>2</sup> This dependence may be expressed by the relation

$$p = \text{funct} (D, v, \rho, \mu, E) \quad (1)$$

where the form of  $\text{funct} (D, v, \rho, \mu, E)$  depends on the shape of the nozzle but is the same for geometrically similar nozzles.

---

<sup>1</sup> For a more complete classification see Part I of Report No. 110 of the National Advisory Committee for Aeronautics, "The Altitude Effect on Air-Speed Indicators."

<sup>2</sup> It is presupposed (a) that the axis of the nozzle is parallel to the direction of motion relative to the medium, (b) that a steady state has been established, and (c) that the medium is homogeneous and undisturbed.



If it were desired to consider the effect on the differential pressure of changing the shape of the tube, a sufficient number of dimensions of the tube to specify these changes should be included among the independent variables in equation (1). The present investigation was not conducted for the purpose of obtaining information of this nature, however. Consequently, only one dimension of the tube, necessary to specify the absolute size, has been included in equation (1), and the following discussion will be understood to apply to nozzles which are geometrically similar.

By means of dimensional reasoning, equation (1) can be rewritten

$$\text{funct} \left( \frac{p}{\rho v^2}, \frac{Dv\rho}{\mu}, \frac{E}{\rho v^2} \right) = 0 \quad (2)$$

or

$$p = \rho v^2 \text{ funct} \left( \frac{Dv\rho}{\mu}, \frac{E}{\rho v^2} \right) \quad (2a)$$

The variable  $\frac{Dv\rho}{\mu}$  is due to the viscosity of the medium which affects the performance of certain types of nozzles at low speeds; whereas the variable  $\frac{E}{\rho v^2}$ , which is present because of the compressibility of the medium, is important only at the higher speeds.

For Pitot tubes,  $p$  is independent of  $\frac{Dv\rho}{\mu}$  within the accuracy of present methods of measurement, as might be expected, since no flow through the tube takes place, once a steady state has been established. The effect of compressibility can be determined analytically for the Pitot tube by making use of comparatively simple and reasonable assumptions.<sup>3</sup> The complete formula for the pressure delivered by a Pitot tube may be written, therefore,

$$p = \rho v^2 \text{ funct} \left( \frac{E}{\rho v^2} \right) \quad (3)$$

In Part I, section 10, and Part II, section 1, of this report the effect of compressibility is discussed further, and it is shown that for the Pitot tube the value of  $\text{funct} \left( \frac{E}{\rho v^2} \right)$  at zero speed does not change by more than 1 per cent for speeds up to approximately 150 miles per hour, but that, above this speed, the magnitude of this effect increases rapidly as  $v$  becomes greater. (See fig. 14.) Since the highest accuracy of calibration which is required of the indicator itself is of the order of 1 per cent of its maximum range, it is customary to neglect the effect of compressibility for the ordinary range of flying speeds, and equation (3) then becomes:

$$p = K\rho v^2 \quad (3a)$$

for Pitot tubes. The constant  $K$  thus introduced into the formula is called the Pitot tube constant and has approximately or exactly the value 0.5, depending on the Pitot tube used.

It is often more convenient, particularly in connection with the calibration of air-speed nozzles and indicators to express  $p$  in terms of head of water, mercury, or whatever liquid is used for the manometers. Equation (3a) may then be written

$$h = \frac{K\rho}{gd} v^2 \quad (3b)$$

by means of the relation

$$p = gdh \quad (4)$$

The form which the general equation (2a) assumes for Venturi tubes has been discussed in Report No. 110 of the National Advisory Committee for Aeronautics. This report was based

<sup>3</sup> "The Theory of the Pitot and Venturi Tubes," by E. Buckingham, Part 2 of Report No. 2 of the National Advisory Committee for Aeronautics, First Annual Report, 1915; and "Development of Air Speed Nozzles," by A. F. Zahm, Report No. 31, Fourth Annual Report, 1918.



on an investigation of the performance of Venturi air-speed pressure nozzles at low speeds and at high altitudes. In Report 110 it was shown that for low values of the variable  $\frac{Dv\rho}{\mu}$  the differential pressure developed by the Venturi was dependent on this variable to a marked degree. It was also shown that the available data covering a speed range of from 30 to 65 miles per hour exhibited no correlation between the performance of the tube and the compressibility. Further evidence of this lack of correlation is presented in Part I, section 10, of the present report. The conclusion which is drawn there, that the effect of the compressibility of the atmosphere on the performance of the Venturi tubes studied in this investigation is negligible over the ordinary range of flying speeds, will be utilized here in order to justify the elimination of the compressibility variable from (2a) for the discussion of this type of tube. The general equation (2a) then reduces to

$$p_1 = \rho v^2 F\left(\frac{Dv\rho}{\mu}\right) \quad (5)$$

or

$$p_1 = K_1 \rho v^2 \phi\left(\frac{Dv\rho}{\mu}\right) \quad (5a)$$

for Venturi and Pitot-Venturi tubes. The reason for writing the particular form (5a) in place of (5) will be made clear in the portion of the next section which deals with the calibration of indicators for use with Venturi tubes. The Venturi constant  $K_1$  is analogous to the Pitot constant  $K$ .

Obviously, (5a) can also be written

$$h_1 = \frac{K_1 \rho}{gd} v^2 \phi\left(\frac{Dv\rho}{\mu}\right) \quad (5b)$$

The form of the function  $\phi$  for a given Venturi tube must be determined before the performance of this tube can be predicted for any given conditions. The data presented in Report 110 showed that  $\phi\left(\frac{Dv\rho}{\mu}\right)$  varies considerably for low values of the argument but is a constant at the higher values of  $\frac{Dv\rho}{\mu}$  for a majority of the Venturi and Pitot-Venturi tubes tested. Unfortunately, errors due to the imperfections of the small low-pressure wind tunnel used in this earlier investigation made it impossible to determine an empirical form for the function  $\phi$  with any degree of accuracy. On this account it was decided to construct a new low-pressure wind tunnel with a larger throat and a greater range of air speeds and to mount it in an altitude chamber where a greater variation of air pressure would be possible. The results obtained from tests in the new wind tunnel are reported in this paper, and the altitude correction is deduced for the two types of air-speed nozzle in most common use in this country, the Navy type and the Army type Zahm Pitot-Venturi nozzles.

### 3. THEORY OF THE CALIBRATION OF AIR-SPEED INDICATORS.

If it were feasible to construct an indicator which would take account of all the variable quantities in equations (3a) and (5a), such an instrument would indicate the true air speed directly, and no corrections would need to be applied, aside from those due to imperfections in the instrument itself. Difficulties in construction and the limitations imposed by the conditions encountered in flight, however, have made it impracticable to construct air-speed instruments of the differential pressure type which will do more than indicate the true air speed for one given set of conditions. For this reason, Pitot-type instruments have been calibrated heretofore in accordance with the relation

$$\text{or} \quad \left. \begin{aligned} p &= K \rho_0 v_1^2 \\ h &= \frac{K \rho_0}{gd} v_1^2 \end{aligned} \right\} \quad (6)$$



where  $K$  has the value  $\frac{1}{2}$  and where  $\rho_0$  is a convenient density chosen as a standard which represents average conditions near sea level.

Similarly the majority of indicators for use with Venturi tubes have been calibrated in accordance with the formula

$$\text{or } \left. \begin{aligned} p_1 &= K_1 \rho_0 v_1^2 \\ h_1 &= \frac{K_1 \rho_0}{g d} v_1^2 \end{aligned} \right\} \quad (6a)$$

where  $K_1$  is the constant value which  $F\left(\frac{Dv\rho}{\mu}\right)$  takes for the higher range of air speeds and which is ordinarily several times greater than the constant  $K$  for the Pitot tube.

It has not been considered necessary to take account of the change in value of  $F\left(\frac{Dv\rho}{\mu}\right)$  at low speeds when Venturi air-speed nozzles have been used on heavier-than-air craft at relatively high speeds and low altitudes, since the range of values of  $\frac{Dv\rho}{\mu}$  for which  $F\left(\frac{Dv\rho}{\mu}\right)$  is constant happens to coincide approximately with the range of flying speeds of such craft for most of the Venturi and Pitot-Venturi nozzles in common use. Consequently the assumption that  $F\left(\frac{Dv\rho}{\mu}\right)$  has the constant value  $K_1$  has been found sufficiently accurate for ordinary conditions of flight as far as heavier-than-air craft were concerned. When, however, Venturi nozzles were applied to the measurement of the relatively low air speeds of lighter-than-air craft, the assumption of a constant value for  $F\left(\frac{Dv\rho}{\mu}\right)$  was at wide variance with facts, and the calibration of the indicators in accordance with equation (6a) permitted errors as great as 20 or 25 per cent in determining the air speed to occur. These errors could have been, and probably were in some instances, reduced materially by the calibration of the indicators according to pressures actually delivered by the nozzle at different speeds for one particular air density. The fact that  $F\left(\frac{Dv\rho}{\rho}\right)$  is a function not only of speed, but also of air density and air viscosity, shows that this procedure did not remove the error, but merely decreased its magnitude.

#### 4. THEORY OF THE ALTITUDE CORRECTION.

From the preceding discussion it can be seen that the correction of the readings of Venturi or Pitot-Venturi air-speed indicators to true air speed involves the solution of the two simultaneous equations

$$p_1 = K_1 \rho v^2 \phi\left(\frac{Dv\rho}{\mu}\right) \quad (3a)$$

and

$$p_1 = K_1 \rho_0 v_1^2 \quad (6a)$$

for  $v$  in terms of the other variables through the elimination of the differential pressure  $p_1$ . Eliminating  $p_1$  gives

$$\left(\frac{v_1}{v}\right)^2 = \frac{\rho}{\rho_0} \phi\left(\frac{Dv\rho}{\mu}\right) \quad (7)$$

Theoretically, the solution of equation (7) for  $v$ , once the form of the function  $\phi$  has been determined, will serve to correct the indicated air speed  $v_1$  for the particular conditions existing at the time when the reading was taken. Practically, however, this procedure is not convenient in general owing to the fact that  $v$  occurs in  $\phi\left(\frac{Dv\rho}{\mu}\right)$  which may prove to have a complicated form. A simpler method for computing the correction will now be derived in which the function to be determined experimentally contains only quantities which are known or which can be computed easily from observations taken during the flight.



By reference to equation (7) it can be seen that the following relation exists

$$v = \text{funct} (D, v_i, \rho, \rho_o, \mu) \quad (8)$$

Equation (8) may be rewritten:

$$\frac{v}{v_i} = \theta \left( \frac{\rho_o}{\rho}, \frac{Dv_i\rho}{\mu} \right) \quad (9)$$

which can be solved directly for  $v$  when the form of the function  $\theta \left( \frac{\rho_o}{\rho}, \frac{Dv_i\rho}{\mu} \right)$  has been determined.

Before this solution can be obtained, three things are necessary: (a) the standard air density  $\rho_o$  for which the indicator was calibrated must be known, (b) the value of the calibration constant  $K_1$  must be determined (in order to compute  $v_i$  for use in this investigation), and (c) an empirical form for  $\theta \left( \frac{\rho_o}{\rho}, \frac{Dv_i\rho}{\mu} \right)$  must be obtained from experiment.

The remainder of Part I of this report will be devoted to this purpose. Part II will be reserved for a more complete discussion of the density, compressibility, and viscosity corrections and for the application of the method just outlined to the data obtained from two types of air-speed nozzles.

#### 5. NOZZLES TESTED IN THIS INVESTIGATION.

The differential pressure air-speed nozzles in most common use are as follows:

United States:

Pitot-Venturi—

Zahm, Navy type.

Modified Zahm, Army type (Oliver).

Toussaint-Lepère (for performance testing).

Great Britain:

Pitot (static openings)—

British standard.

Ogilvie.

France:

Pitot-Venturi—

Toussaint-Lepère.

Venturi (single and double)—

Badin (single throat, static openings).

Badin (double throat without static openings).

Italy:

Venturi—

Badin (double throat).

Germany:

Pitot—

Atmos (static openings).

Venturi (double throat)—

Bruhn (without static openings).

The following tubes were tested in the course of this investigation:

Make.	Serial No.	Identification No.
Zahm Pitot-Venturi (Navy type) <sup>1</sup> .....	330	.....
Do. <sup>1</sup> .....	338	1687
Do. <sup>1</sup> .....	361	B836
Zahm Pitot-Venturi (Army type) <sup>1, 2, 3</sup> .....	327	30
Do. <sup>1</sup> .....	328	B2500
Toussaint-Lepère Pitot-Venturi <sup>1</sup> .....	325	8
Do. <sup>1</sup> .....	363	X4
Do. <sup>3</sup> .....	.....	X9
Badin Venturi, single <sup>1, 2</sup> .....	322	.....
Badin Venturi, double <sup>1</sup> .....	320	.....
Bruhn Venturi, double <sup>1</sup> .....	326	3934
Do. <sup>1</sup> .....	333	1345
Do. <sup>2</sup> .....	370	4898

<sup>1</sup> Low-pressure tests.

<sup>2</sup> Ordinary wind-tunnel tests.

<sup>3</sup> High-speed tests.



It is evident from the preceding that samples of all types of Venturi and Pitot-Venturi tubes in common use for the purpose of air-speed measurement in aeronautics were tested.

The majority of these tubes were tested in the low-pressure wind tunnel. A number were tested in ordinary wind tunnels, and several were tested in the high-speed wind tunnel at McCook Field in order to obtain checks on the work in the low-pressure wind tunnel, to determine the constants of the tubes, and to ascertain to what upper limit the tubes perform in accordance with the simple  $\rho v^2$  law.

#### 6. STANDARD AIR DENSITY.

The standard air density  $\rho_0$  used in calibrating air-speed indicators in the United States is 0.001221 gram per cubic centimeter, corresponding to a barometric pressure of 760 millimeters of mercury and to an air temperature of  $+16^\circ$  centigrade. Whenever either of the expressions "standard conditions" or "standard air density" is used in this report, it will be understood that these values are referred to unless a different meaning is clearly indicated.

Two other standard air densities are necessarily introduced into the discussion. The first of these is the Bureau of Standards wind-tunnel standard, which is involved in the constant of the Pitot tube used to calibrate the static plates of the low-pressure wind tunnel for this

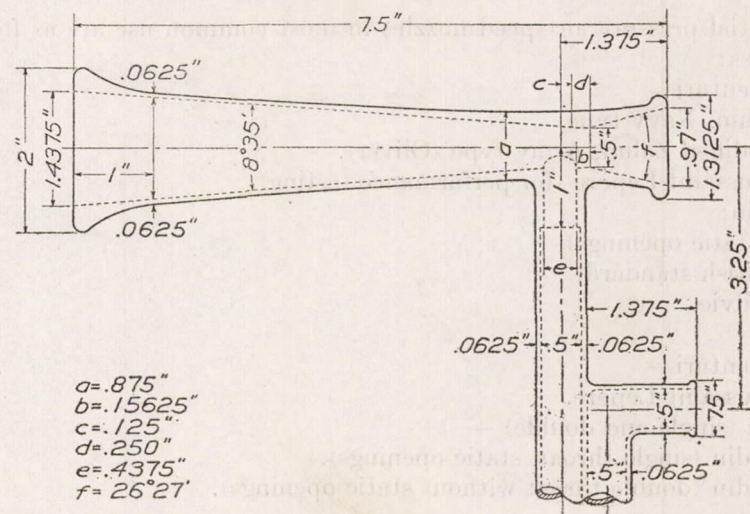


FIG. 1a.—Navy-Zahm Pitot-Venturi.

investigation. This air density is 0.001223 gram per cubic centimeter and corresponds to a barometric pressure of 760 millimeters of mercury and to an air temperature of  $+15.6^\circ$  centigrade. The second of these is the French aircraft performance standard density of 0.001225 gram per cubic centimeter, corresponding to a barometric pressure of 760 millimeters of mercury and to an air temperature of  $+15^\circ$  centigrade.

Where either of these two latter air densities is used in this report its identity is specifically indicated.

#### 7. DETERMINATION OF CONSTANTS OF NOZZLES.

The theoretical performance constant  $K_1$  used in calibrating the indicators was available for only three types of nozzles tested in this investigation—the Navy and Army types of Zahm nozzle and the Bruhn nozzle. Various sources of information were utilized in the attempt to determine representative values of this constant for each of the three types of French nozzle tested. These sources include data from the French laboratories in which the nozzles were calibrated and data from wind tunnel tests conducted at the Bureau of Standards and at McCook Field. These data are presented in detail in the following discussion of the determination of the constant  $K_1$  for each type of tube.

*Zahm nozzle (Navy type).*—In the development of the original Zahm nozzle (see fig. 1a) the pressure-speed relation for the indicators was based on a calibration curve determined



experimentally. A table of pressures corresponding to various air speeds was then made for the use of manufacturers and inspectors of these instruments. It is found, however, that the equation

$$v_i = 17.89\sqrt{h_1} \tag{10a}$$

where  $v_i$  is in miles per hour and  $h_1$  in inches of water, represents this relation quite accurately, as is shown in Table I.

TABLE I.

Air speed (m. p. h.).	Pressure by Zahm plot (inches water).	Pressure from relation $v_i = 17.89\sqrt{h_1}$ (inches water).
20	1.25	1.25
40	5.00	5.00
60	11.23	11.24
80	20.00	20.00
100	31.25	31.24
120	45.00	44.99
140	61.20	61.24
160	80.00	79.99

The constant in equation (10a) corresponds to the standard air conditions of 760 millimeters mercury and +16° centigrade.

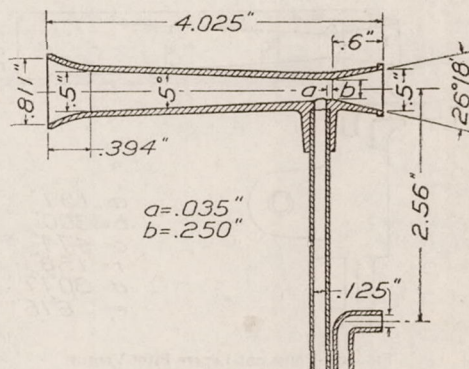


FIG. 1b.—Army-Zahm Pitot-Venturi.

*Modified Zahm nozzle (Army type).*—In the development of the modified Zahm nozzle (see fig. 1b), the attempt was made to design a tube whose performance could be represented by equation (10a).<sup>5</sup>

In computing  $K_1$  for the Zahm tubes, both Army and Navy types, we start with the generally accepted formula

$$v_i = 17.89\sqrt{h_1} \tag{10a}$$

where  $v_i$  is in miles per hour,  $h_1$  is in inches of water, and the standard conditions of 760 millimeters mercury and 16° C. are assumed.

If equation (6a) is written in this form, there results:

$$v_i = \sqrt{\frac{g d}{K_1 \rho_0}} \sqrt{h_1} = C\sqrt{h_1} \tag{6b}$$

Consequently—

$$\sqrt{\frac{g d}{K_1 \rho_0}} = 17.89$$

<sup>4</sup> This is merely another way of writing (6a).

<sup>5</sup> Approximately. The constant was assumed as 17.9 instead of 17.89. The difference is negligible, and equation (10a) will be assumed in this report to apply to indicators for use with both the Army and Navy type Zahm tubes.



In order that the results may be in C. G. S. units, the constant 17.89 should be changed so that in (10a)  $v_i$  shall be in centimeters per second and  $h_i$  in centimeters of water, i. e.

$$v_i = 501.8 \sqrt{h_i}.$$

Equating the expression  $\sqrt{\frac{g d}{K_1 \rho_0}}$  to the constant 501.8 and substituting the numerical values of  $d$  and  $\rho_0$ , we obtain

$$\frac{K_1}{g} = 0.003253$$

or

$$K_1 = 3.188 (g = 980).$$

$\frac{K_1^6}{K}$  then equals 6.38, which is seen to agree well with the low-pressure wind-tunnel data for the Zahm tubes.<sup>7</sup>

*Toussaint-Lepère.*—These air-speed nozzles (see fig. 1c) have been used to some extent by the United States Air Service, both because they are easier to mount ahead of the leading edge

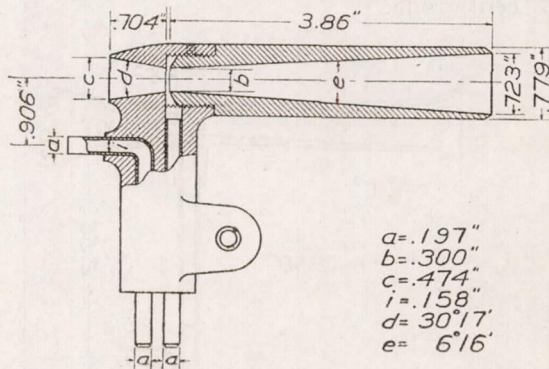


FIG. 1c.—Toussaint-Lepère Pitot-Venturi.

of the airplane than are the Zahm tubes and because the Toussaint-Lepère air-speed recorders have been used in performance testing.

In their manufacture no special conditions are imposed as regards construction tolerances, so, as a result, appreciable differences occur in the dimensions of individual tubes. Consequently, these tubes have no standard calibration curve and their performance varies appreciably. The French practice, therefore, is to calibrate separately each Toussaint-Lepère tube with its corresponding recorder and to determine in this way the performance of each individual outfit.

In spite of the possibility for error thus arising through the method of construction of the tubes, the three Toussaint-Lepère tubes tested in this investigation gave fairly consistent results. On this account a constant based on data for three different tubes has been determined for these nozzles. The first value was obtained from the test, the results of which are tabulated in Table II and in which the air speed was varied from approximately 80 to 285 miles per hour. The remaining two values were obtained from two other tubes tested in the low-pressure wind tunnel at air speeds ranging from approximately 20 to 90 miles per hour. (See figs. 9f and 9g.) In obtaining these three average values, the data obtained at air speeds below 40 miles per hour were discarded, since the viscosity effect was noticeable below these speeds. It was also found

<sup>6</sup>  $K$ , the Pitot tube constant, is  $\frac{1}{2}$ .

<sup>7</sup>  $\frac{K_1}{K} = \frac{p_1}{p}$  for large values of  $\frac{Dv\rho}{\mu}$ . See equation (13a).



that the value of the constant was appreciably higher for the one observation made at a speed above 250 miles per hour, so this value was discarded also.

The data shown in Table II and plotted in figure 2 were obtained from a test made by one of the authors in the high-speed wind tunnel at McCook Field.<sup>8</sup>

TABLE II.—*Toussaint-Lepère, identification No. X9.*

Air speed (m. p. h.).	Pitot head in inches water.	Pitot-Venturi head $h_1$ (inches water).	$\frac{h_1}{h}$	$\frac{Dv\rho}{\mu}$
83.0	3.0	13.1	4.37	22,500
112.7	5.5	24.6	4.48	30,400
153.0	10.0	44.8	4.48	41,000
195.5	16.2	72.0	4.44	52,100
236.2	23.1	103.8	4.50	62,500
268.0	29.6	129.7	4.43	69,900
287.5	33.8	140.5	4.16	74,500

Figure 2 shows that this tube obeys the  $\rho v^2$  law as well as the Pitot does up to at least 250 miles per hour. The falling off in relative performance at the highest speed is probably a correct indication of what happens with this tube, but, owing to the fact that there is only one point which shows this tendency, further evidence is needed.

By substituting in equation (6b) the data from which figures 2, 9f, and 9g, were plotted and then correcting  $C$  for air density by multiplying it by  $\sqrt{\frac{\rho}{\rho_0}}$ , we obtain the values 20.5, 21.1, and

22.1. The average of these values was assumed as characteristic of these tubes, so that the formula which would serve for the calibration of indicators for use with Toussaint-Lepère nozzles is given by

$$v_i = 21.2\sqrt{h_1} \quad (10b)$$

where  $v_i$  is in miles per hour and  $h_1$  is in inches of water.

In determining the constant  $K_1$  for the Toussaint-Lepère nozzle, equation (10b) is first transformed to

$$v_i = 595\sqrt{h_1}$$

where  $v_i$  is in centimeters per second,  $h_1$  is in centimeters of water, and standard conditions are assumed.

$$\text{Then} \quad \sqrt{\frac{g d}{K_1 \rho_0}} = 595;$$

$$\text{whence} \quad \frac{K_1}{g} = 0.00231,$$

$$K_1 = 2.26,$$

$$\text{and} \quad \frac{K_1}{K} = 4.52,$$

which agrees closely with Figure 2.

*Badin single Venturi.*—Both the Badin single and double Venturi nozzles (See figs. 1d and 1e) are adjusted to a standard calibration curve by the process of testing at a given speed (130 kilometers per hour) and then changing slightly, if necessary, the angles of the cones until the tube delivers the standard pressure at that speed within a fraction of a per cent. It is assumed that a series of these tubes giving identical pressures at one particular speed and having a common zero will have exactly the same calibration curve. This is probably true over the ordinary speed range of heavier-than-air craft, but it is extremely doubtful if it is so at the lower

<sup>8</sup> The authors wish to acknowledge the courtesy of the Engineering Division of the Air Service in placing the high-speed wind tunnel at McCook Field at their disposal for several tests which are reported in this paper. The cordial cooperation of the wind-tunnel staff in these tests was of material assistance.



speeds of lighter-than-air craft where the viscosity effect becomes appreciable, as will be shown later in this paper.

The constant  $C$  for the Badin single Venturi tube was obtained from the data shown in Tables III and IV and plotted in Figure 3. The first set of data (Table III) was obtained from an ordinary wind-tunnel test in Bureau of Standards wind tunnel No. 2<sup>9</sup>. The second set (Table IV) was computed from a standard curve furnished upon request by the designer of the nozzle, M. Badin. The agreement of the two sets of data is very good, as can be seen from inspection of Figure 3.

TABLE III.—Badin single Venturi, serial No. 322.

Air speed (m. p. h.).	Pitot head $h$ (centi- meters water).	Venturi head $h_1$ (centime- ters water).	$\frac{h_1}{h}$	$\frac{Dv_p}{\mu}$
16.8	0.333	1.30	3.38	4,600
19.5	.446	1.85	3.59	5,300
22.0	.569	2.25	3.42	6,000
25.3	.756	3.15	3.60	6,900
29.3	1.01	4.35	3.71	8,000
33.7	1.34	6.10	3.94	9,200
38.2	1.71	8.20	4.13	10,400
43.8	2.26	11.70	4.47	12,000
46.7	2.55	13.50	4.58	12,800
49.2	2.85	15.10	4.58	13,400
50.4	3.18	16.40	4.46	13,800
55.9	3.70	20.50	4.79	15,300
60.4	4.50	24.80	4.77	16,500
70.4	6.05	33.20	4.76	19,200
81.2	7.75	43.70	4.89	22,200
89.9	9.52	54.80	4.99	24,600
98.8	11.5	66.20	4.99	27,200
106.8	13.4	77.10	4.98	29,200
111.1	14.5	83.70	5.00	30,300
122.8	17.7	105.70	5.17	33,500
131.8	20.5	122.50	5.19	36,000
144.0	24.4	146.80	5.21	39,300

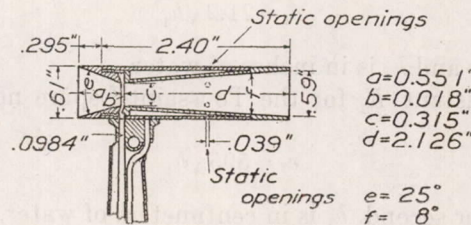


FIG. 1d.—Badin single Venturi.

If  $v_i$  is expressed in centimeters per second and  $h_1$  in centimeters of water, equation (10c) becomes

$$v_i = 568.0 \sqrt{h_1}$$

Following the previous procedure:

$$\sqrt{\frac{g d}{K_1 \rho_0}} = 568.0;$$

whence

$$\frac{K_1}{g} = 0.002539,$$

and

$$K_1 = 2.488.$$

Then

$$\frac{K_1}{K} = 4.98,$$

which is in agreement with Figure 3 and the last eight values in Table IV.

*Badin double Venturi.*—Table V and Figures 1c and 3 illustrate the design and characteristic performance of the Badin double Venturi as given by a calibration curve furnished by M. Badin. As in the case of the Badin single Venturi, the air conditions for which the calibration

<sup>9</sup> The wind-tunnel staff of the Bureau of Standards cooperated in obtaining ordinary wind-tunnel data for a number of nozzles tested in this investigation.

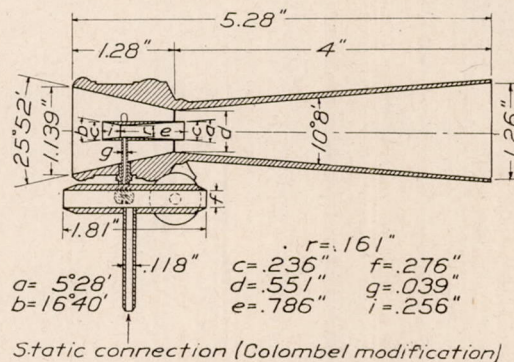


curve was drawn are not known, so the French standard conditions of 760 millimeters mercury and 15° C. were assumed. Comparison of Figure 3 with Figure 9i shows that the low-pressure wind-tunnel tests of Badin nozzle serial No. 320 agree very well with the curve furnished by M. Badin.

TABLE IV.—Badin single Venturi, calculated from curve furnished by Badin.

Air speed (m. p. h.).	Pitot head $h_1$ (centime- ters water).	Venturi head $h$ (centime- ters water).	$\frac{h_1}{h}$	$\frac{Dv_p}{u}$
12.4	0.190	0.3	1.58	3,800
18.6	.433	1.3	3.00	5,600
24.8	.768	2.8	3.65	7,500
31.0	1.200	5.0	4.17	9,400
37.3	1.730	8.0	4.62	11,300
43.5	2.360	11.2	4.75	13,100
49.7	3.080	15.3	4.97	15,000
55.9	3.890	19.7	5.06	16,900
62.1	4.800	24.0	5.00	18,800
74.6	6.930	35.0	5.06	22,500
87.0	9.430	46.8	4.97	26,300
100.0	12.470	60.2	4.83	30,100
111.7	15.580	76.2	4.89	33,700
124.1	19.200	94.5	4.92	37,600

The average value of the constant  $C$  was obtained from data at air speeds varying from 50 to 125 miles per hour. At lower speeds the value increased appreciably. No correction



Static connection (Colombel modification)

FIG. 1e.—Badin double Venturi.

was made for air density, since the air conditions which the curve represented were not given.

The equation which is taken as representing the performance of the Badin single Venturi tube at air speeds above 50 miles per hour is

$$v_1 = 20.25\sqrt{h_1} \quad (10c)$$

where  $v_1$  is in miles per hour and  $h_1$  is in inches of water. Tests at high air speeds indicate that this relation probably holds good at least to speeds of 200 miles per hour.

TABLE V.—Badin double Venturi, calculated from curve furnished by Badin.

Air speed (m. p. h.).	Pitot head $h$ (inches water).	Venturi head $h_1$ (inches water).	$\frac{h_1}{h}$	$\frac{Dv_p}{\mu}$
18.6	0.66	4.5	6.8	5,640
24.8	.88	8.0	9.1	7,520
31.0	1.23	12.8	10.4	9,400
37.3	1.77	19.9	11.2	11,300
43.5	2.42	28.0	11.5	13,200
49.7	3.15	38.0	12.0	15,000
55.9	3.99	48.8	12.2	16,900
62.1	4.81	61.0	12.7	18,800
74.6	6.94	90.3	13.0	22,500
87.0	9.45	126.5	13.4	26,300
99.4	12.32	172.5	14.0	30,100
111.8	15.60	225.0	14.4	33,800



No constant could be determined for this nozzle, as the curves in Figures 3 and 9 show that the value of  $K_1$  was still increasing at the highest air speeds which could be attained.

*Bruhn double Venturi.*—This tube is designed to give a differential pressure 13.6 times as great as that delivered by a standard Pitot tube; in other words, to produce the same differential head of mercury as a Pitot tube would of water.<sup>10</sup> It is stated by W. Hort that this

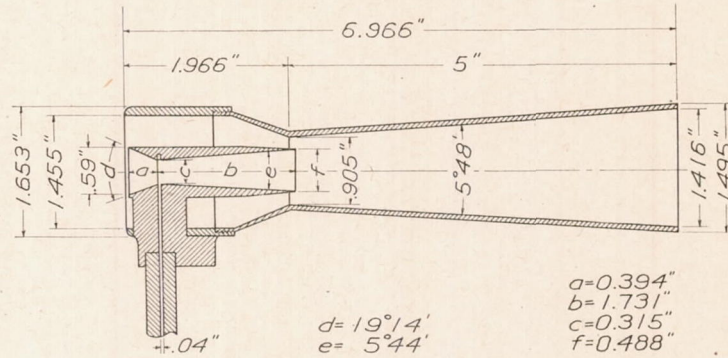


FIG. 1f.—Bruhn double Venturi.

condition is not quite attained in the actual performance of the nozzle, so that the tubes must be calibrated individually. In the course of this investigation, however, a Bruhn tube, serial No. 370, just received from Germany, gave at high speeds almost exactly 13.6 times the pressure delivered by a Pitot tube: hence this relation was assumed to be standard. This tube (serial No. 370) was a new one, whereas the two which were tested in the low-pressure wind

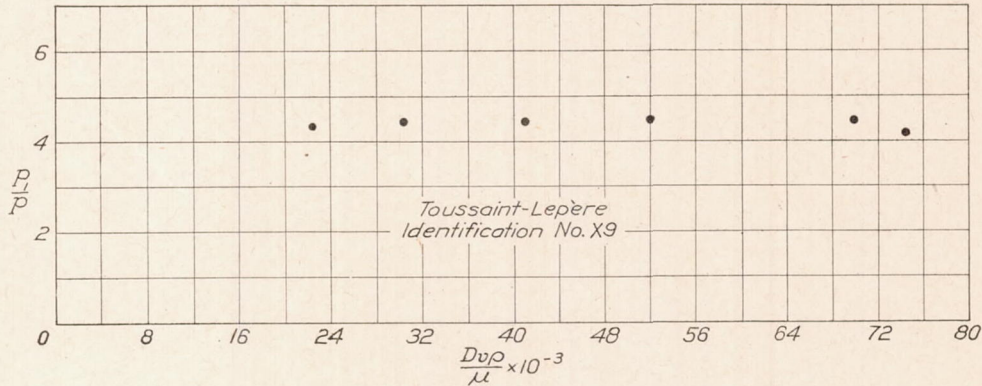


FIG. 2.—Results of tests in ordinary wind tunnel.

tunnel were used during the recent war and showed signs of hard usage. On this account more confidence is placed in the results given by No. 370 than in those given by Nos. 326 and 333. Owing to the fact, however, that No. 370 was received too late to be given tests at reduced pressure in the low-pressure wind tunnel, results for Nos. 326 and 333 are included in order to illustrate the viscosity effect on these tubes. Table VI and Figure 4 give the results obtained in a test of tube No. 370 in wind tunnel No. 2 at the Bureau of Standards.

<sup>10</sup> Ein neues Instrument zur Geschwindigkeitsmessung auf Flugzeugen, W. Hort, Zeitschrift für Flugtechnik und Motorluftschiffahrt, vol. 9, 1918, p. 67.



TABLE VI.—Bruhn double Venturi, serial No. 370.

Air speed (m. p. h.).	Pitot head $h$ (inches water).	Venturi head $h_1$ (inches water).	$\frac{h_1}{h}$	$\frac{Dv\rho}{\mu}$
27.1	0.87	7.8	9.0	7,420
35.5	1.48	14.4	9.7	9,710
47.1	2.62	28.4	10.8	12,900
50.2	2.96	32.8	11.1	13,700
52.4	3.25	36.6	11.2	14,300
58.3	4.01	46.6	11.6	16,000
63.9	4.82	57.8	12.0	17,500
70.2	5.80	70.6	12.1	19,200
76.8	6.94	86.2	12.4	21,000
84.4	8.40	105.4	12.6	23,100
86.0	8.72	112.7	12.9	23,500
91.8	9.95	128.0	13.0	25,100
98.2	11.39	149.6	13.1	26,800
103.2	12.52	166.4	13.3	28,200
104.1	12.76	167.3	13.1	28,400
113.0	15.07	200.8	13.3	30,900
118.5	16.53	223.0	13.5	32,300
123.2	17.88	243.0	13.6	33,700
128.7	19.53	266.0	13.6	35,200
131.4	20.33	277.5	13.6	35,900
134.5	21.32	291.0	13.6	36,800

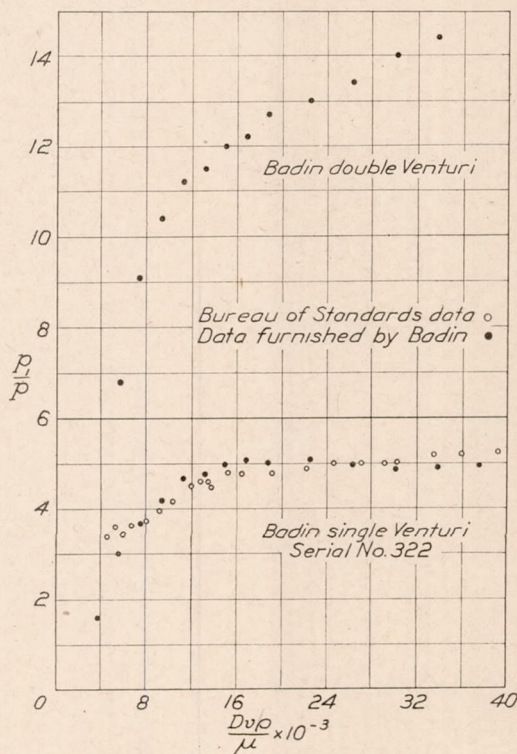


FIG. 3.—Results of tests in ordinary wind tunnel.

The calibration shown in Figure 4 agrees so well with the theoretical value of 13.6 that the ratio  $\frac{K_1}{K}$  for the Bruhn tube will be taken as 13.6.

Then  $K_1 = 6.800$

and  $\frac{K_1}{g} = 0.006939$

The formula for the Bruhn tubes can be written

$$v_1 = 12.28\sqrt{h_1} \tag{10d}$$

where  $v_1$  is in miles per hour,  $h_1$  is in inches of water, and standard conditions are assumed.



The calibration curves plotted in Figure 5 are obtained from the formulas just given except in the case of the Badin double Venturi. This last is obtained from the curve furnished by M. Badin.<sup>11</sup> (See Table V.) The curves computed from the formulas (10a-d) are only approximate at low speeds owing to the viscosity effect, but they are useful for reference purposes.

### 8. DETERMINATION OF FORM OF $\theta \left( \frac{\rho_0}{\rho}, \frac{Dv_i\rho}{\mu} \right)$

In order to determine accurately the form of the function  $\theta \left( \frac{\rho_0}{\rho}, \frac{Dv_i\rho}{\mu} \right)$  for low values of the argument, it was necessary to run a series of tests for each type of tube at low values of the variable  $\frac{Dv\rho}{\mu}$  (or  $\frac{Dv_i\rho}{\mu}$ ). In doing this it makes no difference whether  $v$  is decreased or  $\rho$  is decreased, as far as the value of  $\frac{Dv\rho}{\mu}$  is concerned, but it does make a very appreciable difference

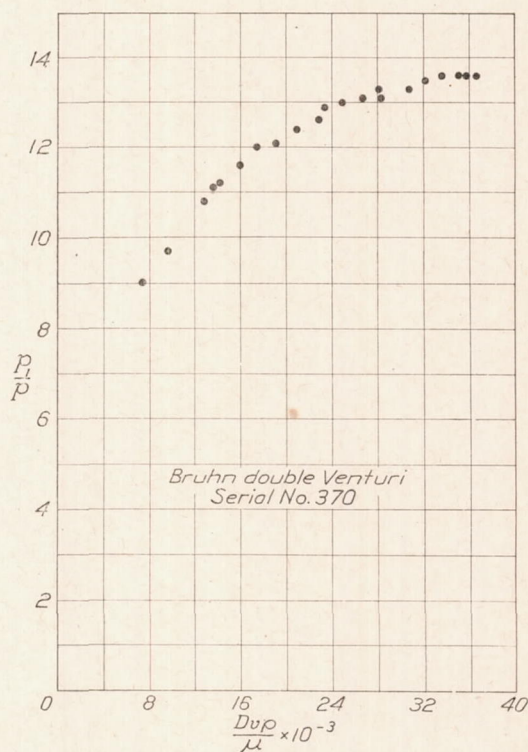


FIG. 4.—Results of tests in ordinary wind tunnel.

in the magnitude of the pressures delivered by the static plate and the tube under test, since these pressures depend on the product  $\rho v^2$ . It can be shown that the pressures obtained when  $\rho$  is decreased are greater than if  $v$  were decreased enough to produce the same change in the value of  $\frac{Dv\rho}{\mu}$ . Thus the use of a low-pressure wind tunnel makes it possible to obtain greater accuracy of measurement at low values of  $\frac{Dv\rho}{\mu}$  than if extremely low speeds were used in an ordinary wind tunnel.

#### DESCRIPTION OF LOW-PRESSURE WIND TUNNEL.<sup>12</sup>

The unusual features of the low-pressure wind tunnel (figs. 6 and 7) used in this investigation warrant a fairly complete description of it. The tunnel was designed to fit in one of the

<sup>11</sup> Since the curve for the Badin double Venturi is obtained from experimental data, it includes the viscosity effect, whereas the other curves, which are plotted from equations (10a-d), do not. This fact explains why the curve for the Badin tube crosses that for the Bruhn tube.

<sup>12</sup> The authors are indebted to the airplane power plant section of the Bureau of Standards for permission to mount the wind tunnel in one of the engine altitude chambers and to the staff of this section for their cooperation in the tests.



new altitude chambers used for testing airplane engines at the Bureau of Standards.<sup>13</sup> The chamber is approximately 14½ feet long by 8 feet wide by 11 feet high. The tunnel was made 11½ feet long, so that a space of about 18 inches was available at each end of the tunnel between the end of the cone and the wall.

The entrance cone was made square in cross section and tapered, as shown in Figure 7, from 32 inches at the entrance to 16 inches at the throat in a distance of 3 feet. A wooden honeycomb was placed at the entrance with one layer of mosquito netting<sup>14</sup> across it. The throat was 18 inches long and was square in cross section. A removable cover to which the Venturi tubes could be attached was set in the top of the throat. The exit cone was made of sheet iron and was 7 feet long, tapering from a circular section 32 inches in diameter at the fan end to a section 16 inches square at the throat.

Since a high air speed was not the primary consideration in the design of this tunnel, no attempt was made to utilize the refinements by which the efficiency of a wind tunnel can be slightly increased, but ease of construction was given the preference.

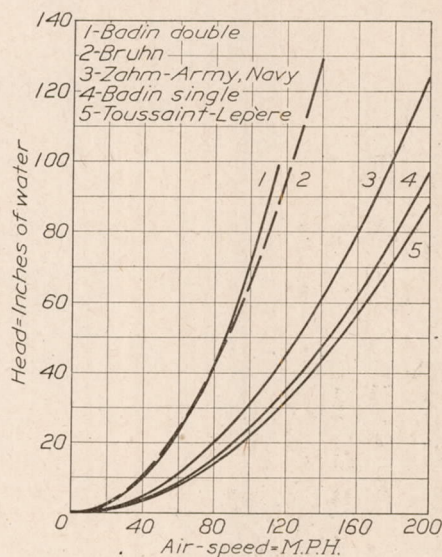


FIG. 5.—Calibration curves for Venturi air-speed nozzles.

A two-blade fan 30 inches in diameter was specially designed and used in this tunnel. It was driven through a belt by a 25-horsepower variable-speed motor. The maximum fan speed attained was about 2,800 r. p. m.

Figure 6 shows the door to the altitude chamber with the fan end of the tunnel just visible. The motor is mounted beneath this end of the tunnel. Outside the chamber on the left of the door are the controller and circuit breaker for the motor. On the right are shown the three manometers used in the tests. Nos. 1 and 2 are inclined benzene manometers having slopes of approximately 0.07 and 0.4, respectively. The third is a vertical U-tube water manometer. The air density inside of the chamber can be computed from the readings of the barometer, shown at the left of the manometer, and the thermometer hanging in the doorway. The thermometer was read through a glass window in the door.

The air speed was measured by means of a static plate. Two static plates were set into one of the side walls of the throat, one near each end. Tests at various barometric pressures showed that the upstream plate (the one nearer the entrance cone) gave more consistent results than the other, so this plate was used throughout the tests.

The static plate was connected to the inclined manometers on account of the small differential pressures involved, particularly at low speeds and high altitudes. In order that a more

<sup>13</sup> The assistance of Mr. Walter Kirby, of the aeronautic instruments section of the Bureau of Standards, in connection with the design of the low-pressure wind tunnel is acknowledged.

<sup>14</sup> To damp time fluctuations of velocity and to produce a more nearly uniform velocity distribution over the cross section of the throat.



open scale might be obtained, the plate was connected at low speeds to the inclined manometer with the smaller slope. At the same time, the Venturi tube under test was connected to the other inclined manometer. Valves were arranged so that, when the benzene in either manometer approached the upper end of the tube, the static plate connection could be shifted quickly to the inclined manometer of greater slope and the Venturi connection to the vertical manometer. This arrangement proved very satisfactory.

The inclined manometers were calibrated against a water column which was read by means of a cathetometer. As the relation between the manometer reading and the corre-

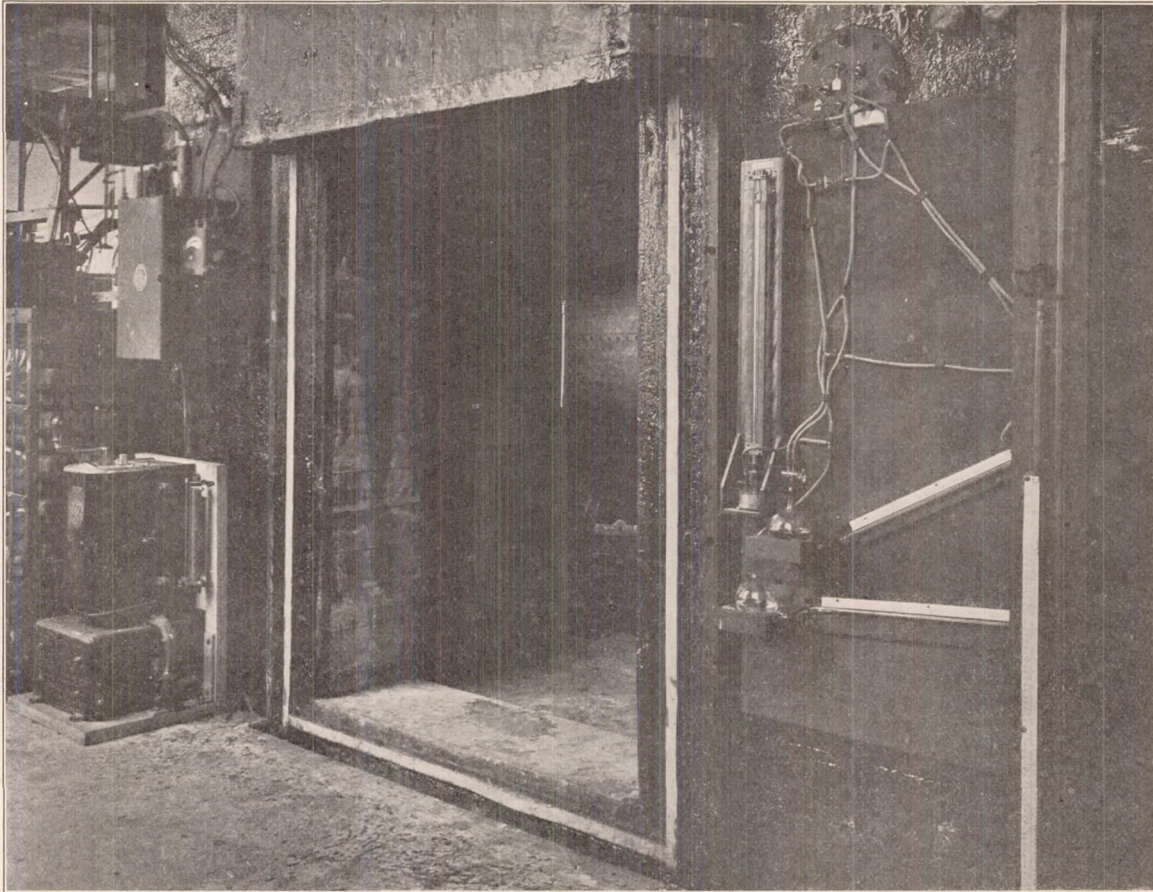


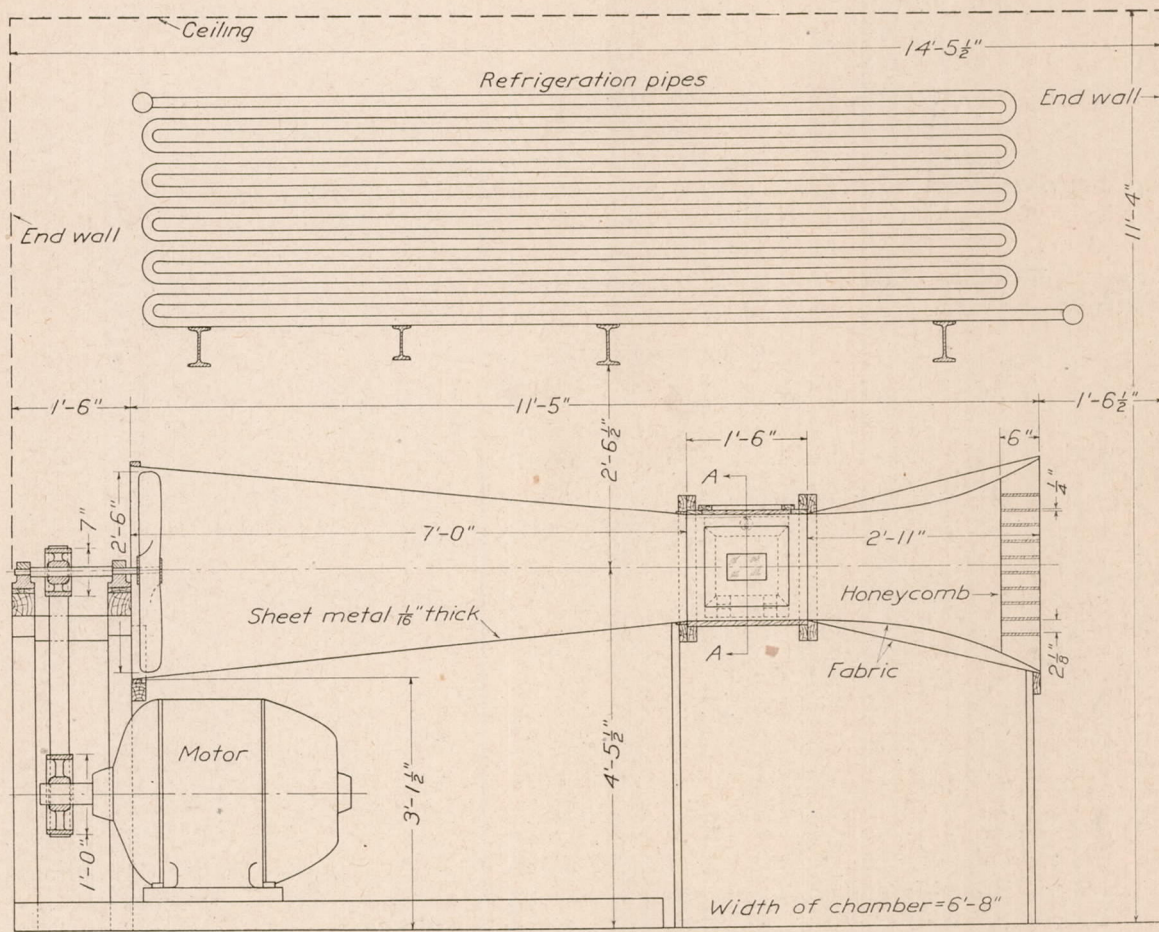
FIG. 6.—Altitude chamber.

sponding vertical head of water is not generally linear at low pressures, it was necessary to plot the ratio of vertical head of water to manometer reading against manometer reading for each manometer and to refer to these plots in reducing the observations.

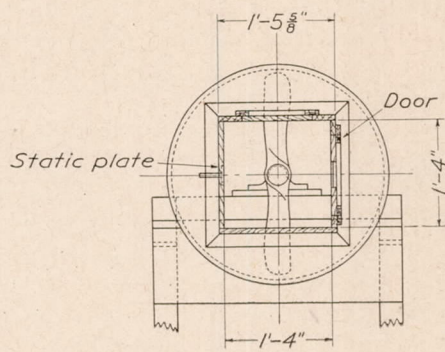
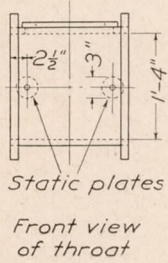
The static plate was calibrated against a standard Pitot tube at various barometric pressures. Upon plotting the pressure delivered by the static plate against that delivered by the standard Pitot, it was found that a straight line resulted for each given air density, and that changing the air density resulted in altering the slope of this line slightly. This fact made it possible to change the static plate readings to standard Pitot readings very easily for any given pressure. The ratio of the Pitot pressure to the corresponding static plate pressure was determined for calibrations at four different air densities ranging from about 0.0004 to 0.0012 gram per cubic centimeter. When these ratios were plotted against air density<sup>15</sup> they were found

<sup>15</sup> This ratio would undoubtedly prove to be a function of  $\frac{Dv\rho}{\mu}$ ; but since the air temperature was practically the same in all of the tests,  $v$  and  $\rho$  were the only independent variables.

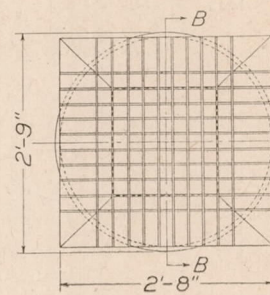




Section on B-B



Section on A-A



End view

FIG. 7.—Low-pressure wind tunnel, Bureau of Standards.



to lie quite closely along a straight line. (Fig. 8.) Consequently the most probable straight line was determined for the four points and was used in reducing observations.

To determine the true air speed at the throat of the tunnel the following method was used: The pressure delivered by the static plate was determined from the readings of the inclined manometer and the calibration curve for the manometer. From the static plate calibration (fig. 8) the corresponding pressure for the standard Pitot tube was obtained. Then the air speed was computed from equation (3b).

Since, in the case of a Pitot-Venturi nozzle, both the Pitot and the Venturi can not be placed at the center of the tunnel simultaneously, it was necessary to determine the velocity distribution over the cross section of the throat of the tunnel. This was done over an area 8 inches square symmetrical with respect to the center of the tunnel and with the sides horizontal and vertical. This area was sufficient to include the openings of all the tubes tested.

The velocity distribution was studied over the range of barometric pressures used in the tests which follow. Almost without exception the variation was within 1 per cent. In no case was this value greatly exceeded.

#### LOW-PRESSURE WIND-TUNNEL TESTS.

Samples of all types of Venturi and Pitot-Venturi tubes in common use were tested in the low-pressure wind tunnel. Particular attention was paid to the Zahm tubes, both Army and Navy types, since these tubes are the most commonly used in the United States.

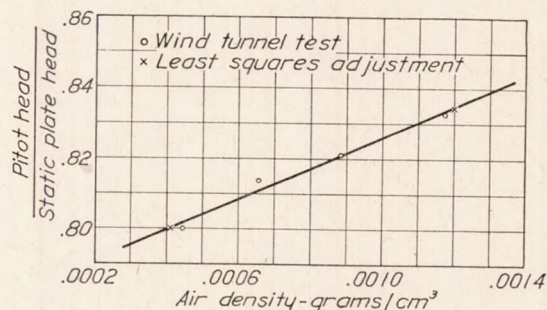


FIG. 8.—Calibration curve for static plate. Low-pressure wind tunnel.

Photographs of these tubes are shown in Figure 1, N. A. C. A. Report No. 110, already referred to. Longitudinal cross sections are shown in Figures 1a to 1f of this present report.

The tube to be tested was mounted at the center of the throat of the tunnel. The differential pressure delivered by the tube was measured for speeds varying from approximately 15 to 90 miles per hour. This process was repeated for a series of air pressures from full atmospheric pressure to approximately 250 millimeters of mercury. Under these conditions it was found possible to reach values of  $\frac{Dv_p}{\mu}$  as low as 1,500, using C. G. S. units and taking  $D$  as 1 centimeter. These are distinctly lower values than were obtained with the old low-pressure wind tunnel, with which it was found impossible to reach values of  $\frac{Dv_p}{\mu}$  lower than 4,000.

The readings taken during the tests included the pressures delivered by the static plate and the tube under test and the air temperature and pressure inside of the chamber. With the Pitot-Venturi tubes the lower end of the manometer was connected to the Pitot and the upper to the Venturi. Since the Badin single Venturi has static openings, the lower end of the manometer was connected to these. A small auxiliary static tube<sup>16</sup> sometimes used with the Badin double Venturi was attached to the nozzle and connected to the lower end of the manometer when this nozzle was tested. The Bruhn tube has no static pressure holes, so the lower end of the manometer was connected to the downstream static plate.

A sample table of data and computations is given below for Zahm nozzle serial No. 330. Owing to the amount of space required to tabulate the data and computations for all the tubes, only the plots resulting from the data are given for the other tubes. (See figs. 9a-k.)

<sup>16</sup> Colombel modification.



TABLE VII.—Zahm nozzle, serial No. 330.

1	2	3	4	5	6	7	8	9	10	11	12	13	14
Run No.	Bar. pres. $B$ (cm. of Hg.).	Temp. $t$ ( $^{\circ}C$ .)	Pit. pres. $h$ (cm. of water).	Pit.-Vent. pres. $h_1$ (cm. of water).	Air density $\rho$ (gms./cm. <sup>3</sup> ).	Air viscosity $\mu$ (gms./cm.sec.).	True air speed $v$ (cm./sec.).	Indicated air speed $v_i$ (cm./sec.).	$\frac{h_1}{h}$	$\frac{Dv}{\rho}$	$\frac{Dv_i}{\rho}$	$\frac{v}{v_i}$	Relative density $\frac{\rho}{\rho_0}$ .
1	755	24.3	0.505	2.58	0.001179	0.0001855	915	805	5.11	5,820	5,120	1.135	0.966
			.710	3.34			1,080	920	4.70	6,870	5,850	1.175	
			1.395	7.92			1,520	1,410	5.68	9,670	8,970	1.080	
			2.040	11.5			1,840	1,700	5.64	11,700	10,800	1.080	
			2.82	16.6			2,160	2,050	5.89	13,700	13,000	1.055	
			3.76	22.9			2,500	2,400	6.09	15,900	15,300	1.040	
			4.98	31.0			2,880	2,800	6.22	18,300	17,800	1.030	
			5.53	34.2			3,030	2,940	6.19	19,300	18,700	1.030	
			6.13	37.9			3,190	3,090	6.19	20,300	19,700	1.030	
			6.67	41.4			3,360	3,230	6.21	21,400	20,500	1.040	
			7.69	49.4			3,570	3,530	6.42	22,700	22,500	1.010	
			9.39	60.9			3,950	3,920	6.49	25,100	24,900	1.010	
			8.23	51.9			3,700	3,620	6.31	23,500	23,000	1.020	
			7.18	44.4			3,450	3,340	6.19	21,900	21,200	1.035	
			6.29	37.0			3,230	3,050	5.88	20,500	19,400	1.060	
5.76	35.4	3,090	2,990	6.15	19,600	18,900	1.035						
3.25	19.6	2,320	2,220	6.04	14,800	14,100	1.045						
1.915	10.8	1,780	1,650	5.64	11,300	10,500	1.080						
.565	2.74	970	830	4.85	6,170	5,280	1.170						
.510	2.45	920	785	4.80	5,850	4,990	1.170						
.430	2.06	925	720	4.79	4,900	3,820	1.285						
.805	4.51	1,270	1,070	5.60	6,740	5,670	1.190						
2.31	13.80	2,150	1,870	5.98	11,400	9,920	1.150						
4.13	24.9	2,870	2,500	6.03	15,200	13,200	1.145						
5.55	34.4	3,330	2,940	6.20	17,600	15,600	1.135						
7.96	49.9	3,990	3,550	6.27	21,200	18,800	1.125						
5.82	36.4	3,410	3,030	6.26	18,100	16,100	1.125						
3.61	21.9	2,680	2,350	6.07	14,200	12,500	1.140						
1.265	7.11	1,590	1,340	5.62	8,380	7,070	1.185						
.445	2.06	945	720	4.63	4,980	3,800	1.310						
.355	1.49	925	615	4.20	4,050	2,690	1.505						
.460	1.93	1,050	700	4.22	4,600	3,070	1.500						
1.900	10.65	2,140	1,640	5.61	9,380	7,180	1.305						
3.77	22.4	3,020	2,380	5.94	13,200	10,400	1.270						
6.52	39.9	3,970	3,170	6.12	17,400	13,900	1.250						
4.22	25.4	3,190	2,530	6.02	14,000	11,100	1.260						
2.12	12.4	2,260	1,770	5.85	9,900	7,760	1.275						
.480	2.05	1,080	720	4.27	4,730	3,150	1.500						
.355	1.45	925	605	4.09	4,050	2,650	1.530						
.280	1.10	940	525	3.93	3,170	1,770	1.790						
.425	1.75	1,160	665	4.12	3,910	2,240	1.745						
1.200	6.10	1,940	1,240	5.08	6,540	4,180	1.565						
2.83	16.0	2,980	2,020	5.65	10,100	6,810	1.485						
5.19	30.8	4,040	2,790	5.94	13,600	9,400	1.450						
3.48	20.4	3,310	2,270	5.86	11,100	7,660	1.460						
1.620	11.8	2,260	1,730	7.28	7,620	5,830	1.305						
.370	1.55	1,080	625	4.19	3,640	2,110	1.730						
.275	1.05	930	515	3.82	3,130	1,740	1.905						
.195	.630	905	400	3.23	2,290	1,010	2.260						
.205	.670	930	410	3.27	2,350	1,040	2.270						
.315	1.165	1,150	540	3.70	2,910	1,370	2.160						
.615	2.45	1,610	785	3.97	4,070	1,990	2.100						
.720	3.09	1,740	880	4.29	4,400	2,230	1.980						
1.390	6.74	2,420	1,300	4.85	6,120	3,290	1.860						
1.87	9.66	2,800	1,560	5.16	7,080	3,950	1.795						
2.58	14.4	3,290	1,910	5.58	8,320	4,830	1.725						
3.00	15.9	3,550	2,000	5.30	8,980	5,060	1.775						
4.04	23.4	4,120	2,430	5.80	10,400	6,150	1.695						
3.49	19.9	3,830	2,240	5.71	9,690	5,670	1.710						
2.87	15.8	3,470	2,000	5.51	8,780	5,060	1.735						
2.16	11.8	3,010	1,730	5.46	7,620	4,380	1.740						
2.06	11.6	2,940	1,710	5.64	7,440	4,330	1.720						
1.33	6.58	2,360	1,290	4.95	5,970	3,270	1.830						
.695	2.94	1,710	860	4.23	4,330	2,180	1.990						
.275	.960	1,080	490	3.49	2,730	1,240	2.205						
.210	.670	940	410	3.19	2,380	1,040	2.290						
.195	.630	905	400	3.23	2,290	1,010	2.260						
.060	.185	550	215	3.08	1,180	460	2.560						
.120	.365	775	305	3.08	1,660	652	2.540						
.145	.485	850	350	3.34	1,820	750	2.425						
.250	.870	1,120	470	3.48	2,400	1,010	2.385						
.410	1.61	1,430	640	3.93	3,060	1,370	2.240						
.575	2.47	1,700	790	4.30	3,640	1,690	2.150						
1.00	5.12	2,240	1,140	5.12	4,790	2,430	1.965						
.540	2.27	1,650	755	4.20	3,530	1,615	2.185						
.360	1.32	1,340	575	3.67	2,870	1,230	2.330						
.175	.590	935	385	3.37	2,000	824	2.430						
.140	.445	835	335	3.18	1,790	717	2.495						
.075	.225	613	240	3.00	1,310	514	2.550						
2	627	23.3	0.505	2.58	.000982	.0001851	915	805	5.11	5,820	5,120	1.135	.804
			.710	3.34			1,080	920	4.70	6,870	5,850	1.175	
			1.395	7.92			1,520	1,410	5.68	9,670	8,970	1.080	
			2.040	11.5			1,840	1,700	5.64	11,700	10,800	1.080	
			2.82	16.6			2,160	2,050	5.89	13,700	13,000	1.055	
			3.76	22.9			2,500	2,400	6.09	15,900	15,300	1.040	
			4.98	31.0			2,880	2,800	6.22	18,300	17,800	1.030	
			5.53	34.2			3,030	2,940	6.19	19,300	18,700	1.030	
			6.13	37.9			3,190	3,090	6.19	20,300	19,700	1.030	
			6.67	41.4			3,360	3,230	6.21	21,400	20,500	1.040	
			7.69	49.4			3,570	3,530	6.42	22,700	22,500	1.010	
			9.39	60.9			3,950	3,920	6.49	25,100	24,900	1.010	
			8.23	51.9			3,700	3,620	6.31	23,500	23,000	1.020	
			7.18	44.4			3,450	3,340	6.19	21,900	21,200	1.035	
			6.29	37.0			3,230	3,050	5.88	20,500	19,400	1.060	
5.76	35.4	3,090	2,990	6.15	19,600	18,900	1.035						
3.25	19.6	2,320	2,220	6.04	14,800	14,100	1.045						
1.915	10.8	1,780	1,650	5.64	11,300	10,500	1.080						
.565	2.74	970	830	4.85	6,170	5,280	1.170						
.510	2.45	920	785	4.80	5,850	4,990	1.170						
.430	2.06	925	720	4.79	4,900	3,820	1.285						
.805	4.51	1,270	1,070	5.60	6,740	5,670	1.190						
2.31	13.80	2,150	1,870	5.98	11,400	9,920	1.150						
4.13	24.9	2,870	2,500	6.03	15,200	13,200	1.145						
5.55	34.4	3,330	2,940	6.20	17,600	15,600	1.135						
7.96	49.9	3,990	3,550	6.27	21,200	18,800	1.125						
5.82	36.4	3,410	3,030	6.26	18,100	16,100	1.125						
3.61	21.9	2,680	2,350	6.07	14,200	12,500	1.140						
1.265	7.11	1,590	1,340	5.62	8,380	7,070	1.185						
.445	2.06	945	720	4.63	4,980	3,800	1.310						
.355	1.49	925	615	4.20	4,050	2,690	1.505						
.460	1.93	1,050	700	4.22	4,600	3,070	1.500						
1.900	10.65	2,140	1,640	5.61	9,380	7,180	1.305						
3.77	22.4	3,020	2,380	5.94	13,200	10,400	1.270						
6.52	39.9	3,970	3,170	6.12	17,400	13,900	1.250						
4.22	25.4	3,190	2,530	6.02	14,000	11,100	1.260						
2.12	12.4	2,260	1,770	5.85	9,900	7,760	1.275						
.480	2.05	1,080	720	4.27	4,730	3,150	1.500						
.355	1.45	925	605	4.09	4,050	2,650	1.530						
.280	1.10	940	525	3.93	3,170	1,770	1.790						
.425	1.75	1,160	665	4.12	3,910	2,240	1.745						
1.200	6.10	1,940	1,240	5.08	6,540	4,180	1.565						
2.83	16.0	2,980	2,020	5.65	10,100	6,810	1.485						
5.19	30.8	4,040	2,790	5.94	13,600	9,400	1.450						
3.48	20.4	3,310	2,270	5.86	11,100	7,660	1.460						
1.620	11.8	2,260	1,730	7.28	7,620	5,830	1.305						
.370	1.55	1,080	625	4.19	3,640	2,110	1.730						
.275	1.05	930	515	3.82	3,130	1,740	1.905						
.195	.630	905	400										



In Table VII, columns 1, 2, and 3 are self-explanatory.

Column 4 gives the Pitot pressures corresponding to the air speeds and air densities existing in the throat of the tunnel when the observations were made. Actually, as has already been explained, these pressures were determined indirectly by measuring the static pressure drop in the throat of the tunnel by means of a static plate connected to an inclined benzene manometer. The readings of the inclined manometer were then changed to vertical heads of water by means of the calibration curve for the manometer. These heads of water, which were for the static plate, were then changed to the corresponding heads for the standard Pitot by means of the curve shown in Figure 8. The heads thus determined are those given in column 4 and are related to the true air speed  $v$  by equation (3b).

Column 5 gives the differential pressures delivered by the Zahn tube. These pressures were obtained by reducing the inclined manometer readings to vertical head of water or reading directly from the vertical water U-tube, according to which manometer was used.

The air densities existing in the chamber at the time when the observations were made are given in column 6. They are computed from the formula

$$\rho = \rho_0 \frac{BT_0}{B_0T} \quad (11)$$

where  $\rho_0 = 0.001221$  gram per cubic centimeter for the standard conditions  $t_0 = 16^\circ\text{C}$ . ( $T_0 = 289^\circ$ ) and  $B_0 = 760$  millimeters mercury.

Sutherland's formula, given below, was used for the determination of the air viscosities given in column 7.

$$\mu = \mu_0 \frac{1 + \frac{119.4}{273}}{1 + \frac{119.4}{T}} \sqrt{\frac{T}{273}} \quad (12)$$

where  $\mu_0$  was taken as 0.0001733 gram per centimeter per second at  $0^\circ\text{C}$ .

Values of the true air speed  $v$  are given in column 8. These are computed from the equation:

$$h = \frac{K}{g} \frac{\rho}{d} v^2 \quad (3b)$$

The value of  $\frac{K}{g}$  is obtained from the equation for the standard Pitot:

$$v = 28.313 \sqrt{h} \quad (10e)$$

where  $v$  is in miles per hour and  $h$  is in centimeters of water. To obtain  $v$  in centimeters per second, we multiply the constant 28.313 by 44.70 and obtain

$$v = 1266 \sqrt{h}.$$

Now

$$\sqrt{\frac{gd}{K\rho_0}} = 1266$$

and  $\rho_0 = 0.001223$  gram per cubic centimeter, since the constant 28.313 corresponds to the wind-tunnel standard conditions of 760 millimeters of mercury and  $15.6^\circ\text{C}$ .

Whence

$$\frac{K_1}{g} = 0.0005102$$

or

$$K = 0.5000 \quad (g = 980).$$



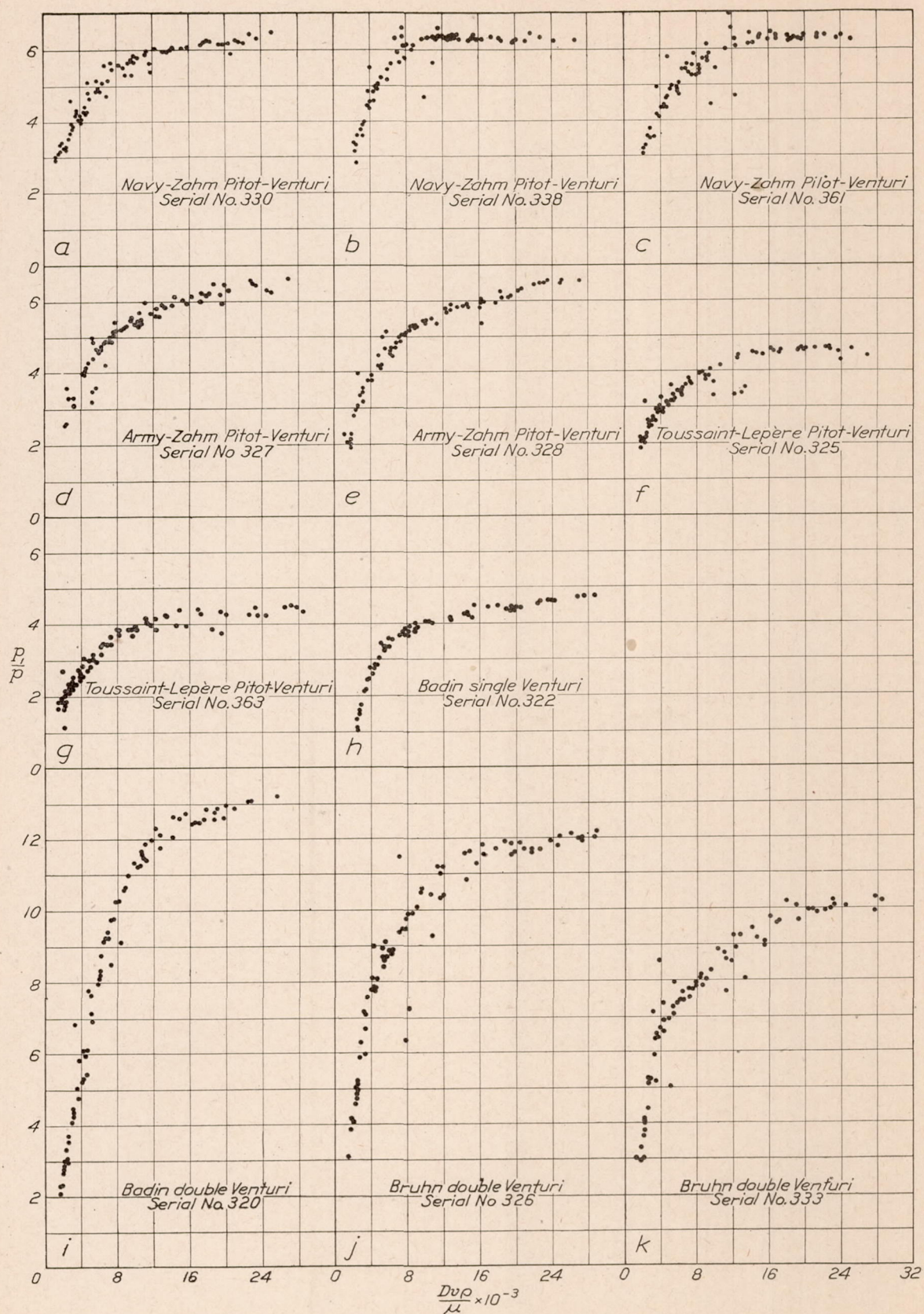


FIG. 9.—Results of tests in low-pressure wind tunnel.



This value of  $K$  agrees within the limits of accuracy of these computations with the value of  $K$  from the theoretical Pitot formula

$$h = \frac{\rho v^2}{2gd} = \frac{K\rho v^2}{gd}$$

In this formula  $K = \frac{1}{2}$ . Consequently, for the purpose of computing  $\frac{p_1}{p}$ , there is no need of correcting the heads delivered by the standard Pitot used in this investigation to the values which would have been obtained from a Pitot whose performance was in accordance with the theoretical Pitot formula.

Column 9 gives values of the indicated air speed  $v_1$  computed from

$$h_1 = \frac{K_1 \rho_0}{g} v_1^2 \quad (6a)$$

in which  $\frac{K_1}{g} = 0.003253$  (for Zahm tubes) and the values of  $h_1$  are taken from column 5.

Columns 10, 11, 12, and 13 are the plotting tables. Columns 10 and 11 are used to furnish the plot of  $\frac{h_1}{h}$  or  $\frac{p_1}{p}$  against  $\frac{Dv\rho}{\mu}$ . The values of the variable  $\frac{Dv\rho}{\mu}$  are computed from the values of  $\rho$ ,  $\mu$ , and  $v$  found in columns 6, 7, and 8, respectively,  $D$  being taken as 1 centimeter, since C. G. S. units are used. The choice of  $D$  is purely arbitrary, since it represents any corresponding linear dimensions of a series of geometrically similar tubes; for example, the throat diameter or the length of the tube. Owing to the fact that, except for several groups of two or three identical tubes each, the ones used in this investigation were not geometrically similar, there is no restriction whatsoever upon  $D$ , and so it is arbitrarily chosen as 1 centimeter for all the tubes. This means that the curves for the different tubes can not be compared among the themselves as far as abscissæ are concerned. In fact, if the tubes were geometrically similar we should obtain the same curve for all the tubes, provided the  $D$ 's were taken proportional to the sizes of the tubes and the roughness of the surfaces was in this same proportion.

Since

$$h = \frac{\rho v^2}{2gd}$$

the ordinates of this curve are twice those in the corresponding plots in N. A. C. A. Report No. 110, where  $\frac{\rho v^2}{gd}$  was used. That arrangement is more logical from the purely physical standpoint, but the present arrangement is deemed better for this report, since the ordinate is a direct measure of the ratio of the pressure delivered by the Venturi (or Pitot-Venturi) tube to that given by a Pitot tube<sup>17</sup> for different values of  $\frac{Dv\rho}{\mu}$ . It also gives the ratio of  $\frac{K_1}{K}$  for the tubes, since

$$h = \frac{K\rho v^2}{gd} \quad (3b)$$

and

$$h_1 = \frac{K_1\rho v^2}{gd} \phi\left(\frac{Dv\rho}{\mu}\right) \quad (5b)$$

from which it follows that

$$\frac{h_1}{h} = \frac{K_1}{K} \phi\left(\frac{Dv\rho}{\mu}\right) \quad (13)$$

<sup>17</sup> This ratio is sometimes called the *efficiency* of the Venturi tube.



For sufficiently great values of  $\frac{Dv\rho}{\mu}$ ,

$$\phi\left(\frac{Dv\rho}{\mu}\right) = 1$$

and

$$\frac{h_1}{h} = \frac{K_1}{K} \quad (13a)$$

for these values.

In the region where (13a) holds, the tube follows the  $\rho v^2$  law.

Figure 9 contains the data for determining the form of the function  $\theta\left(\frac{\rho_0}{\rho}, \frac{Dv_1\rho}{\mu}\right)$  for the different types of nozzles investigated. The data are prepared for this purpose in columns 12 and 13 of Table VII for Navy type Zahm nozzle No. 330. The relative density given in column 14 is used in computing values of  $\frac{v}{v_1}$  from equations (17) and (18).

#### 9. PERFORMANCE OF VENTURI NOZZLES AT VERY HIGH SPEEDS.

As far as can be determined from the available data, the efficiency  $\frac{K_1}{K}$  for each of the Venturi tubes tested in this investigation remains constant for a considerable range of values of  $\frac{Dv\rho}{\mu}$  above the region where the viscosity of the air affects the performance of the tubes. As the value of  $\frac{Dv\rho}{\mu}$  continues to increase, however, a point is reached where this ratio begins to decrease once more. This decrease in efficiency possibly may be due to the compressibility of the air, but this has not been proved as yet.

A brief discussion will be given here of the performance at high speeds of the nozzles tested in this investigation in order that the upper limit of the range over which these tubes obey the  $\rho v^2$  law may be estimated.

*Zahm, Army and Navy.*—In Part II of Report 110, Figure 7, are plotted the data from tests of an Army Zahm tube in the wind tunnel of the Aerotechnic Institute at St. Cyr. Assuming standard conditions and computing the speed corresponding to the highest values of  $\frac{Dv\rho}{\mu}$  given there, the value of 150 miles per hour results. There is no indication from the plot that the speed at which the efficiency of the tube decreases has been reached.

Further corroboration is obtained from the following results obtained by one of the authors from a test made in the wind tunnel at McCook Field in December, 1919.

TABLE VIII.—Army Zahm, serial No. 327.

Air speed (m. p. h.).	Pitot head $h$ (centimeters water).	Pitot- Venturi head $h_1$ (centimeters water).	$\frac{h_1}{h}$	$\frac{Dv\rho}{\mu}$
37.8	1.78	9.40	5.28	11,400
46.7	2.72	16.25	5.98	14,000
73.9	6.86	45.7	6.66	22,200
88.8	9.91	63.0	6.36	26,800
100.9	12.70	81.8	6.44	30,800
116.7	17.02	113.0	6.64	35,100
131.5	21.59	143.0	6.62	39,600
148.7	27.69	180.3	6.52	44,800



These results are plotted in Figure 10.

Tests conducted by the Engineering Division of the Air Service at McCook Field indicate that the formula

$$V = C\sqrt{h} \text{ (with } \rho \text{ constant)}$$

represents the performance of the Army type Zahm tube from the lower speeds of heavier-than-air craft up to 200 miles per hour.<sup>18</sup>

No high-speed data on Navy type Zahm tubes are available for this report. Only experiment can determine whether this type of nozzle will perform in accordance with the  $\rho v^2$  law to as high a speed as does the Army type; and before it is used at the higher flying speeds, its performance at these speeds should be carefully investigated.

*Toussaint-Lepère.*—Figure 2 and Table II show the results obtained from a test of a Toussaint-Lepère nozzle in the high-speed wind tunnel at McCook Field. This nozzle does not appear to be affected appreciably by compressibility up to speeds of at least 240 miles per hour.

*Badin single Venturi.*—Table III and Figure 3 show that there is no decrease in the efficiency of the Badin nozzles up to air speeds of approximately 145 miles per hour. Tests

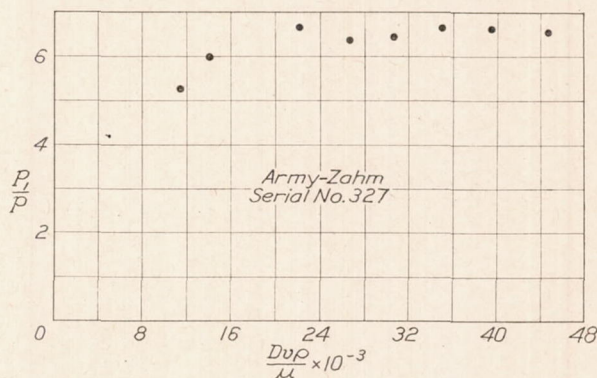


FIG. 10.—Results of tests in ordinary wind tunnel.

conducted by the Engineering Division of the Air Service at McCook Field indicate that the efficiency of this type of tube does not decrease until speeds higher than 200 miles per hour have been attained.

*Badin double Venturi.*—At the highest air speeds reached in this investigation, the performance of this nozzle was affected by air viscosity. Consequently the region in which the tube obeys the  $\rho v^2$  law was not reached in this investigation.

*Bruhn double Venturi.*—Tests conducted by the Engineering Division of the Air Service at McCook Field indicate that the efficiency of the Bruhn tube starts to decrease at a speed between 150 and 180 miles per hour and falls off rapidly at speeds above this. If the values of  $\frac{Dv_p}{\mu}$  corresponding to these speeds are computed for the air conditions on which Table VI and Figure 4 are based (760 millimeters mercury and  $+16^\circ$  C.), 45,000 and 54,000 result. Consequently, it may be expected that the curve in Figure 4 would take on a negative slope at some point between values of  $\frac{Dv_p}{\mu}$  of 45,000 and 54,000, had observations been extended as far as this.

#### 10. DISCUSSION OF DATA.

*Accuracy and range of data.*—Comparison of Figure 11 (a and b) of this report with Figure 4 of Report 110 shows clearly the superiority of the data obtained in the new low-pressure wind tunnel over those from the old one. The curves are quite clearly defined and cover a greater

<sup>18</sup> Information as to the performance at high speeds of several of the types of air-speed nozzle tested in this investigation was furnished through the courtesy of the McCook Field instrument section of the Engineering Division, Air Service.



range of values of  $\frac{Dv\rho}{\mu}$  than do the old ones. This fact makes it possible to show more conclusively than was done in Report 110 that there is no measurable correlation between the ratio  $\frac{h_1}{h}$  and either the density or the compressibility.

*Air density.*—In Figure 11a are plotted the data for Navy type Zahm Pitot-Venturi serial No. 338. The values of  $\frac{h_1}{h}$  corresponding to high air densities are plotted as full circles, while open circles are used for values of  $\frac{h_1}{h}$  corresponding to low densities. In distinguishing between high and low air densities, the arithmetical average of all the densities involved in the low-pressure wind tunnel tests of this tube was taken and those values greater than this average value called high; those less called low. Where the density for a particular run was practically the same as the average density, the points determined by this run were not plotted.

*Compressibility.*—In the same way points corresponding to high and low values of the com-

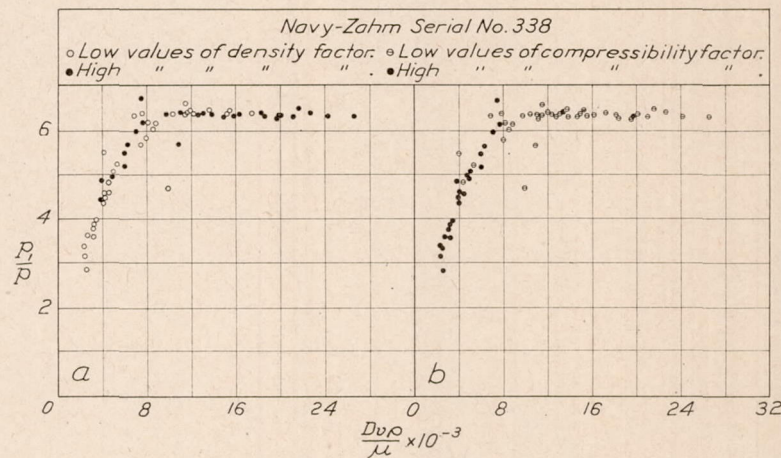


FIG. 11.—Effect of density and compressibility.

pressibility variable  $\frac{E}{\rho v^2}$  are plotted in Figure 11b. For purposes of computing values of this variable,  $E$  was replaced by its equivalent,  $\kappa B$ . No correlation between the performance of this nozzle and the compressibility could be detected for the range of values of  $\frac{Dv\rho}{\mu}$  shown in this plot. This range corresponds to a speed range of from 10 to 90 miles per hour approximately.

Still further evidence of this lack of correlation which, although not decisive, tends to confirm the conclusion that the compressibility effect on the performance of Venturi tubes is negligible over the ordinary range of flying speeds is to be found in the data given in Table II and plotted in Figure 2 of this report. These data were obtained from the test of a Toussaint-Lepère Pitot-Venturi tube in the high-speed wind tunnel at McCook Field. The differential pressure delivered by this tube was measured for speeds up to approximately 285 miles per hour. Inspection of this plot shows that the ratio of the differential pressure  $p_1$  of the Venturi to the Pitot pressure  $p$  is constant within the limits of experimental error between values of  $\frac{Dv\rho}{\mu}$  of 28,000 and 68,000, corresponding to the approximate air speeds at sea level of 100 and 240 miles per hour, respectively. Below this speed range the change in value of the ratio is due to viscosity. The effect of compressibility is included in the Pitot pressure  $p$ . The fact, then, that the ratio  $p_1/p$  remains constant for this particular tube over the range above stated indicates the possibility that the effect of compressibility on the Venturi tube is to increase the suction which it delivers in the same proportion as the Pitot pressure is increased owing to this same cause. This can be



seen from the fact that the effective differential pressure produced by a Pitot-Venturi tube is equal to the numerical sum of the Pitot pressure and the Venturi suction; i. e., the ratio  $p_1/p$  can be written

$$\frac{p_1}{p} = \frac{s+p}{p} = \frac{s}{p} + 1 \quad (14)$$

Now the only way in which the quantity  $s/p + 1$  can remain constant is for the ratio  $s/p$  to remain constant. Consequently since it is known that compressibility increases  $p$ ,  $s$  must be increased numerically in the same proportion by the same effect.

The evidence thus presented showing an apparent lack of correlation between the performance of Venturi air-speed nozzles and the compressibility of the air is utilized in the present

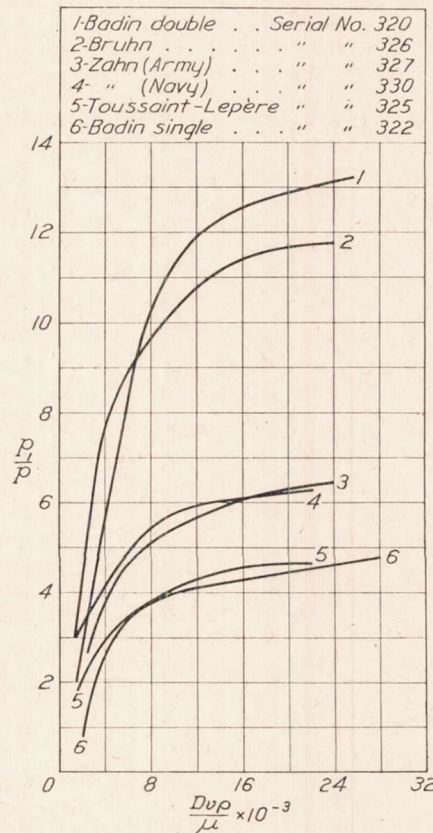


FIG. 12.—Characteristic curves showing viscosity effect. Low-pressure wind tunnel.

paper as a basis for the assumption that the effect of compressibility on the performance of the air-speed nozzles discussed in this paper does not exceed the effect on a Pitot tube and so can be neglected over the ordinary range of flying speeds. This effect requires further experimental investigation.

*Hysteresis.*—In some of the plots of the data obtained in the low-pressure wind tunnel a scattering of points occurs in the region of sharpest curvature. This suggested the possible existence of a small hysteresis loop there similar to that found in the case of pipe lines where turbulent flow changes to stream-line flow. If such a loop existed it would mean that, for the

corresponding range of  $\frac{Dv\rho}{\mu}$ , the differential pressure delivered by the tube would not be determinate unless it was known which side of the loop was being followed. An investigation of this feature, however, gave negative results—no hysteresis could be detected.



*Comparison of viscosity effects on different types of tubes.*—Perhaps the most noticeable feature of the curves shown in Figure 9 and in Figure 12 is the marked viscosity effect upon the double Venturi tubes as contrasted with the single Venturi and the Pitot-Venturi tubes. The underlying cause of this has not been ascertained, but it has been found that the magnitude of the effect for single or double Venturi tubes is measured by the ordinate  $\frac{p_1}{p}$  when  $\phi\left(\frac{Dvp}{\mu}\right)=1$ . The discussion of the limiting values of  $\frac{p_1}{p}$  will make the reason for this clearer.

It is interesting to compare the form of the curve obtained for the Navy type Zahm nozzle with that for the Army type. Examination of Figure 9 (a to e inclusive) shows that the Navy-type tube follows the  $\rho v^2$  law to somewhat lower values of  $\frac{Dvp}{\mu}$  than does the Army type.

This is mainly the result of the larger throat in the Navy type Zahm nozzle. If the tubes were geometrically similar, then by choosing the  $D$  for each tube proportional to the diameter the two curves could be compared and, in fact, would coincide. Now the tubes are not quite similar and so can not be compared directly, but the Navy-type tube has a throat twice the diameter of that of the Army type. Consequently, it would be assumed that, since  $D$  was taken as 1 for each tube, the Navy-type tube would perform in accordance with the  $\rho v^2$  law down to lower values of  $\frac{Dvp}{\mu}$  than would the other.

*Limiting value of  $p_1/p$ .*—Examination of the curves obtained for Venturi tubes, single and double, indicates that the prolongation of these curves would pass through or very near the origin of coordinates. If it were known to be true that as  $\frac{Dvp}{\mu}$  approached zero  $p_1/p$  also approached zero, the discrepancies from this assumed relation could be readily attributed to the difficulty of obtaining accurate data for these low values. It is obviously unsafe to infer what form  $\phi\left(\frac{Dvp}{\mu}\right)$  may take for very small values of the argument, but as far as observations could be extended, the indications were that  $p_1/p$  approached zero as  $\frac{Dvp}{\mu}$  approached zero.

The curves obtained for the Pitot-Venturi tubes are observed to point in a general way toward the value  $\frac{p_1}{p}=1$  for  $\frac{Dvp}{\mu}=0$ . They thus corroborate the conclusions drawn from the Venturi curves, since:

$$\frac{p_1}{p}=1+\frac{s}{p} \quad (14)$$

Now as  $\frac{Dvp}{\mu}$  approaches zero,  $s/p$  approaches zero as has already been observed. Consequently, for Pitot-Venturi tubes, as far as observations were carried

$$\frac{p_1}{p} \doteq 1 \text{ as } \frac{Dvp}{\mu} \doteq 0$$

*Critical pressure-ratio curves.*—The magnitude of the viscosity effect for each type of tube is shown in Figure 13 (a to e). In plotting these curves, the point was first chosen (in fig. 9) where, as nearly as could be determined, the viscosity effect ceased to be appreciable; i. e., where the curve became horizontal. Then for the value of  $\frac{Dvp}{\mu}$  corresponding to this point, values of  $\rho$  and  $\mu$  corresponding to a series of United States standard air altitudes (see Table IX) were substituted and the resulting equation solved for  $v$ . In this way a series of air speeds was obtained corresponding to a series of altitudes. By plotting these speeds against the corresponding altitudes a curve is obtained which is called the "critical pressure-ratio" curve for the tube in question. It shows for each altitude the speed below which the performance of the tube is



affected by viscosity. The other curves are obtained in the same way except that the values of  $\frac{Dv_p}{\mu}$  are selected for which the efficiency of the tube has decreased 10, 20, 30, and 40 per cent below its maximum value. The curves are then computed for the same altitudes as was done for the critical pressure-ratio curve and with the same assumptions as to standard conditions. In connection with these curves it should be remembered that a given percentage error in the efficiency or pressure-ratio involves an error in the indicated speed of only half that amount.

*Comparison of curves for same type of nozzles.*—One feature of the wind-tunnel data which might have been made more striking by the inclusion of other tests is the variation in the shape

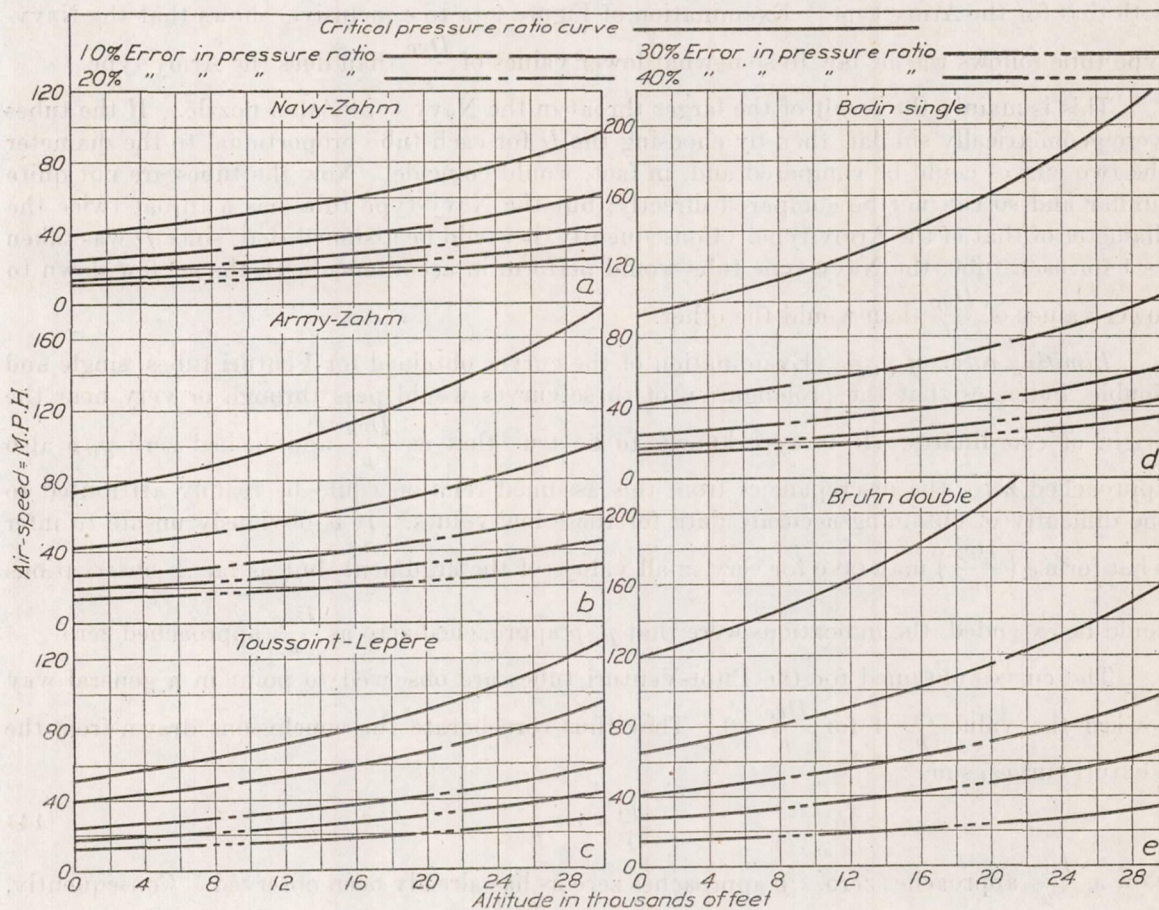


FIG. 13.—Viscosity effect.

of the curves obtained for different tubes of the same kind, tubes which were as nearly alike as they could be made under conditions of quantity production. The results obtained for the three Navy type Zahm nozzles, shown in Figure 9 (a to c), tested in this investigation illustrate this quite well. Although these three curves probably would be found to give the same calibration within less than 1 per cent at the high speeds, there are found appreciable differences at the lower speeds. Nozzle No. 330 is a copper-deposited tube, while nozzles Nos. 338 and 361 are made of cast aluminum. Owing to the fact that Nos. 338 and 361 were made by a process different from that by which No. 330 was made, it might be expected that a greater difference would be found between the curve for No. 330 and that for either Nos. 338 or 361 than would be found in comparing No. 338 with No. 361. The difference between the curves for No. 338 and No. 361 is sufficient, however, to show that apparently insignificant differences in construction may affect the calibration curve appreciably at low speeds. This being the case, it is clearly



impossible to measure low speeds accurately with a Venturi tube unless the tube is given a careful individual calibration.

This fact is significant in connection with the calibration of the Badin nozzles. It is the custom to test these tubes at one fixed speed and to adjust the differential pressure which the tube delivers at that speed to within 0.5 centimeter of the standard pressure by making slight alterations in the shape of the cones. It is assumed that if the calibration curves for these Venturis coincide at two points they will coincide throughout. This assumption unquestionably would be true provided the tubes performed in accordance with equation (3a). Since the tubes perform according to equation (5a) instead and it has been shown that  $\phi \left( \frac{Dv\rho}{\mu} \right)$  may be affected seriously by apparently insignificant differences in the tubes, it is very doubtful whether the assumption is justifiable. It may be satisfactory, however, for the higher speeds.

*Effect of rough or dirty throat.*—The lower the speed at which turbulent flow still persists the greater will be the range over which the tube will perform according to the  $\rho v^2$  law. A slight roughness, therefore, or any other feature which tends to increase turbulence, may be an advantage, provided it does not decrease the efficiency of the tube appreciably at the higher speeds. The fact that dirtying the throat of a Venturi tube increases its efficiency at low speeds and decreases it at high speeds has been noted on several occasions by other experimenters. This phenomenon can easily be explained by the assumption that approximately stream-line flow exists at low speeds and turbulent flow at high speeds.



impossible to measure low speeds accurately with a Venturi tube unless the tube is given a careful individual calibration.

The fact is significant in connection with the calibration of the Balm nozzle. It is the custom to test these tubes at one fixed speed and to adjust the differential pressure which the tube delivers at that speed to within 0.5 centimeter of the standard pressure by making slight alterations in the shape of the cone. It is assumed that if the calibration curves for these tubes are correct at two points they will coincide throughout. This assumption unquestionably would be true provided the tubes performed in accordance with equation (2a), since the tubes

perform normally to equation (2a) instead and it has been shown that  $\frac{V_{obs}}{V_{theor}}$  may be affected seriously by apparently insignificant differences in the tubes, it is very doubtful whether the assumption is justifiable. It may be satisfactory, however, for the higher speeds.

Effect of rough weather. The lower the speed at which turbulent flow still persists the greater will be the range over which the tube will perform according to the law. A slight roughness in the cone or any other feature which tends to increase turbulence may be an advantage provided it does not decrease the efficiency of the tube appreciably at the higher speeds. The fact that during the flight of a Venturi tube in a stream the efficiency at low speeds and turbulence at high speeds has been noted on several occasions by other experimenters. This phenomenon can easily be explained by the assumption that approximately stream-line flow exists at low speeds and turbulent flow at high speeds.



## REPORT No. 156.

### THE ALTITUDE EFFECT ON AIR SPEED INDICATORS—II.

#### PART II.

#### THE ALTITUDE CORRECTION.

##### 1. INTRODUCTION.

Part II of this report is devoted to a discussion of the correction of air-speed indicator readings for compressibility, density, and viscosity, to the determination of suitable empirical forms of the function  $\theta \left( \frac{\rho_0}{\rho}, \frac{Dv_i \rho}{\mu} \right)$  for the Navy Zahm and Army Zahm Pitot-Venturi nozzles, and to the arrangement of the values of the density and viscosity corrections in a form suitable for use.

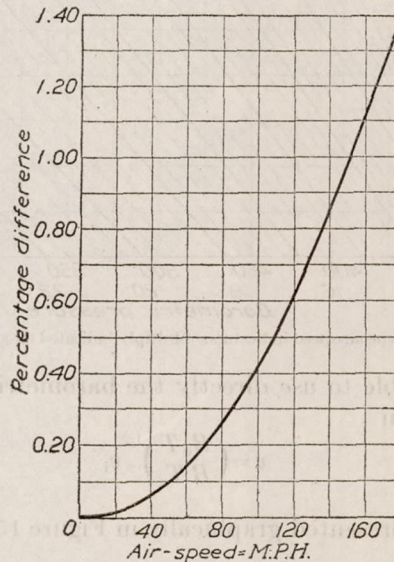


FIG. 14.—Effect of compressibility on Pitot tube pressures.

##### 2. THE COMPRESSIBILITY CORRECTION FOR PITOT NOZZLES.

The effect of compressibility on Pitot tubes can be computed by methods indicated in Reports Nos. 2 (Pt. II) and 31 of the National Advisory Committee for Aeronautics. Figure 14 shows the theoretical effect of compressibility on Pitot tubes. The curve is based on the data given by Zahm (Rept. No. 31). There is some uncertainty as to the accuracy of the theoretical results owing to approximations introduced in the treatment. The indicated speed is slightly too high, if, as is customary, equation (6a) is used as the basis of the calibration of the indicator.

##### 3. THE COMPRESSIBILITY CORRECTION FOR VENTURI NOZZLES.

The effect of compressibility upon the performance of Venturi tubes has not yet been determined, as the discussion in Part I of this report has shown. The uncertainties involved in the assumptions which are required for a theoretical analysis are so great that the result is



mainly of academic interest. In the present state of our knowledge regarding this question, it is probably safe to assume that the effect of compressibility on the performance of the Venturi air-speed nozzles in common use is negligible over the ordinary range of flying speeds at the present time, but this conclusion should not be extended to include speeds greater than, say, 200 miles per hour until it has been verified experimentally for such speeds.

#### 4. THE DENSITY CORRECTION FOR PITOT NOZZLES.

Equations (3a) and (6) represent the relations connecting the true air speed with the reading of a Pitot type indicator. By eliminating  $p$  from these two equations we obtain

$$v = \left( \frac{\rho_0}{\rho} \right)^{1/2} v_i \text{ OR } v = \frac{v_i}{\sqrt{r}}. \quad (15)$$

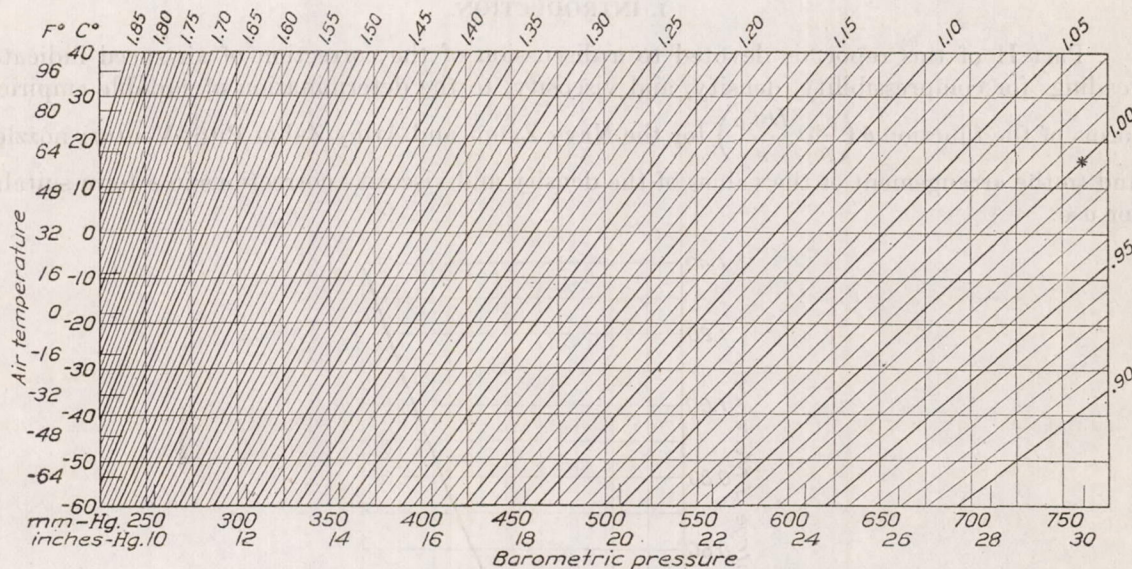


FIG. 15.—Correction factors for Pitot type air-speed indicators. Multiply indicated air speed by factor obtained from this chart.

If it is considered preferable to use directly the barometric pressure and the temperature, equation (15) may be rewritten

$$v = \left( \frac{B_0 T}{B T_0} \right)^{1/2} v_i \quad (15a)$$

The factor  $\left( \frac{B_0 T}{B T_0} \right)^{1/2}$  is represented graphically in Figure 15 which may be used in correcting the readings of air-speed indicators of the Pitot type for density.

#### 5. THE DENSITY CORRECTION FOR VENTURI NOZZLES.

The density correction to air speeds measured by indicators of the Venturi type is expressed by equation (15) for the range of values of  $\frac{Dv\rho}{\mu}$  over which the Venturi obeys the  $\rho v^2$  law. In general, however, a viscosity correction must also be made. These two corrections are applied simultaneously by means of the method which is developed in this paper.

#### 6. VISCOSITY CORRECTION FOR VENTURI NOZZLES.

It was shown in Part I, section 4, of this report that the solution of

$$\frac{v}{v_i} = \theta \left( \frac{\rho_0}{\rho}, \frac{Dv_i\rho}{\mu} \right) \quad (9)$$

for  $v$  furnished a method of correcting the readings of Venturi and Pitot-Venturi air-speed indicators for altitude.



For sufficiently great values of  $\frac{Dv_i\rho}{\mu}$  the ratio  $\frac{v}{v_i}$  is unaffected by viscosity and equation (9) must then take on the form of equation (15)

$$\frac{v}{v_i} = \left(\frac{\rho_0}{\rho}\right)^{1/2} \quad (15)$$

But equation (9) can always be written

$$\frac{v}{v_i} = \psi_1\left(\frac{\rho_0}{\rho}\right)\psi_2\left(\frac{\rho_0}{\rho}, \frac{Dv_i\rho}{\mu}\right) \quad (9a)$$

where  $\psi_1\left(\frac{\rho_0}{\rho}\right)$  may be given any desired form. Consequently it may be specified arbitrarily that  $\psi_1\left(\frac{\rho_0}{\rho}\right)$  shall be of the form  $\left(\frac{\rho_0}{\rho}\right)^2$  given by equation (15). Equation (9a) may now be written

$$\frac{v}{v_i} = \left(\frac{\rho_0}{\rho}\right)^{1/2} \psi\left(\frac{\rho_0}{\rho}, \frac{Dv_i\rho}{\mu}\right) \quad (16)$$

the subscript (2) being omitted since it is no longer needed. For sufficiently high values of  $\frac{Dv_i\rho}{\mu}$ ,

$$\psi\left(\frac{\rho_0}{\rho}, \frac{Dv_i\rho}{\mu}\right) \text{ is equal to } 1.$$

An empirical form of equation (16) will now be determined for the Zahm nozzles, Army and Navy types, tested in this investigation.

In Figure 16 are plotted values of  $\frac{v}{v_i}$  against  $\frac{Dv_i\rho}{\mu}$  for various values of  $\rho$  from Table VII for Navy Zahm tube serial No. 330 and from similar data plotted in Figure 9 for the other tubes. The points represent the experimental data. The form of  $\psi\left(\frac{\rho_0}{\rho}, \frac{Dv_i\rho}{\mu}\right)$  best fitting the data obtained from the three Zahm Navy type nozzles was found to be

$$\left[1 + 0.36 \left(\frac{\rho_0}{\rho}\right)^{1/2} e^{-0.00018 \frac{\rho_0}{\rho} Z}\right]$$

where

$$Z = \frac{Dv_i\rho}{\mu}$$

so that equation (16) assumes the form

$$\frac{v}{v_i} = \left(\frac{\rho_0}{\rho}\right)^{1/2} \left[1 + 0.36 \left(\frac{\rho_0}{\rho}\right)^{1/2} e^{-0.00018 \frac{\rho_0}{\rho} Z}\right] \quad (17)$$

(Zahm, Navy type.)

The form of equation (16) best fitting the data for the two Army Zahm tubes tested in this investigation was found to be

$$\frac{v}{v_i} = \left(\frac{\rho_0}{\rho}\right)^{1/2} \left[1 + 0.41 \left(\frac{\rho_0}{\rho}\right)^{1/2} e^{-0.00017 \frac{\rho_0}{\rho} Z}\right] \quad (18)$$

(Zahm, Army type.)

The form of  $\psi\left(\frac{\rho_0}{\rho}, \frac{Dv_i\rho}{\mu}\right)$  is assumed the same for both the Army and Navy type tubes: the differences are taken care of by varying the constants.

The full lines in Figure 16 represent equations (17) and (18) computed for the values of  $\rho$  for which the experimental data were obtained. It will be seen that the computed values from the equations agree with the experimental values very well indeed.



Figures 17a and 17b show the correction curves obtained by plotting equations (17) and (18), respectively. Curves were plotted for densities varying from 0.0004 to 0.0014 gram per cubic centimeter, which covers a sufficient range to include any observations which may be obtained in ordinary flying or in performance testing. It will be observed that the value of the term  $\left[0.36 \left(\frac{\rho_0}{\rho}\right)^{1/2} e^{-0.00018 \frac{\rho_0}{\rho} Z}\right]$  in equation (17) or the corresponding term in equation (18) decreases very rapidly as  $Z$  increases and that when this term becomes negligible, equations (17) and (18) both reduce to equation (15) which is used to correct air-speed readings for density.

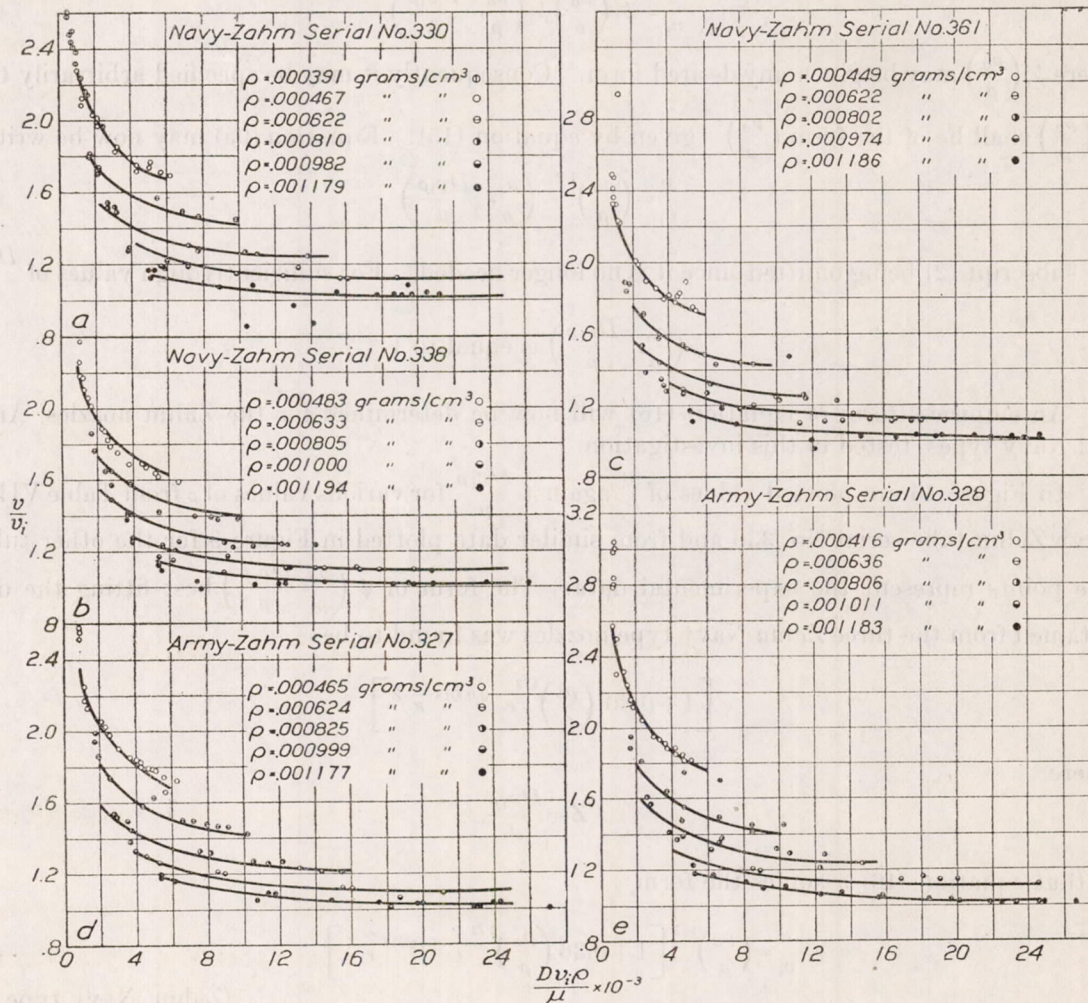


FIG. 16.—Experimental data for determination of  $\Psi \left( \frac{\rho_0}{\rho}, \frac{Dv_i \rho}{\mu} \right)$ .

This is illustrated graphically in Figures 17a and 17b by the curves becoming horizontal. If these horizontal portions of the curves were continued horizontally until they cut the axis of  $\frac{v}{v_i}$ , they would represent the density correction as given by equation (15). The curvature is due to the viscosity correction. The curves corresponding to the lowest densities are continued to values of  $\frac{Dv_i \rho}{\mu}$  corresponding to  $v = 200$  miles per hour upon the assumption that United States standard air conditions exist. The other curves are horizontal beyond the limits of the plot, and so the values of the correction factor can be taken from the edge of the sheet.

The correction curves in Figures 17a and 17b are suitable for performance testing where the necessary observations can be taken during flight and the true air speeds computed later in



the office. Owing to the work incidental to computing the value of  $\frac{Dv_i \rho}{\mu}$ , these curves are not suitable for use in the air. For such use and, in particular, use on dirigible airships, a special set of curves has been prepared in which constant values of  $B$  and  $T$  have been assumed. Any deviation from these conditions will cause an error in determining the true air speed, but by proper interpolation, this error can be kept much smaller than that incurred by ignoring the viscosity effect.

These curves which are suitable for use on dirigible airships are illustrated in Figure 18. They are computed from equation (17) with United States standard air (Radau air) conditions assumed. (See Table IX.) That is, by assuming  $B$  and  $T$ , we can plot  $\frac{v}{v_i}$  against  $v_i$ . In order to allow for all possible variations of  $B$ ,  $T$ , and  $v_i$  it would be necessary to make use of four-dimensional space or to construct a family of surfaces in three-dimensional space, since there are four variables,

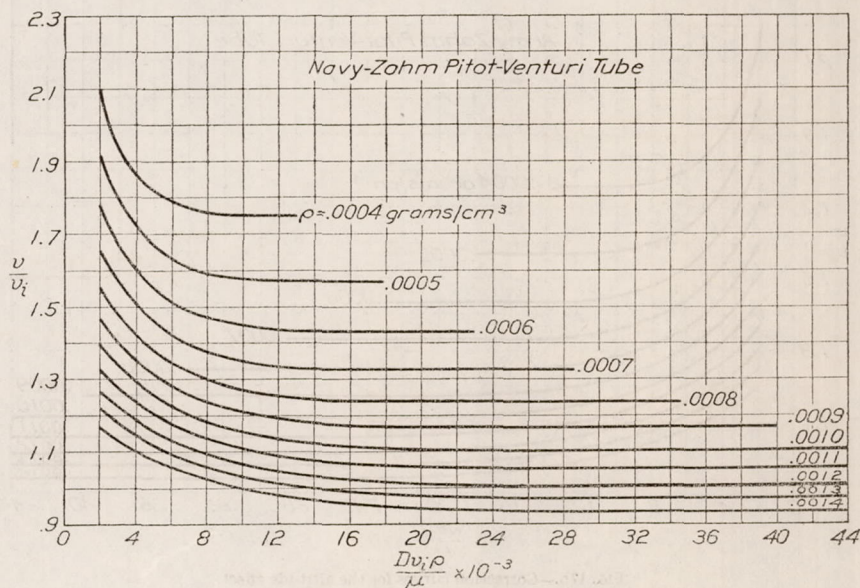


FIG. 17a.—Correction curve for the altitude effect.

$B$ ,  $T$ ,  $v_i$ , and  $\frac{v}{v_i}$ . This is, of course, out of the question for use in the air where conservation of space and ease of use are so important. The scheme adopted was to plot families of curves for four values of  $t$ ,  $+40^\circ$ ,  $+20^\circ$ ,  $0^\circ$  and  $-20^\circ$  C,  $\frac{v}{v_i}$  being plotted against  $v_i$ . The curves of any one family are plotted for suitable values of  $B$  covering the range of pressures which dirigible airships in their present state of development are likely to experience. The values of  $B$  assumed vary from 750 to 400 millimeters of mercury corresponding to isothermal altitudes of approximately 350 feet and 17,000 feet, respectively. The range of  $v_i$  was taken from 5 miles per hour to 100 miles per hour, which should be ample for present purposes.

The correction curves shown in Figure 18 were computed from equation (17) for the Navy-type Zahm nozzles. These curves may be used, however, for both Army and Navy type tubes since the largest error thus introduced into the correction factor is not over 3 per cent. (This is at extremely low speeds.) The corrections for the Army tubes are slightly greater where viscosity is appreciable than are those given in Figure 18.



In order to use the correction curves shown in Figures 17a and 17b it is necessary to compute the value of  $\frac{Dv_i\rho}{\mu}$  from the observed quantities  $v_i$ ,  $B$ , and  $t$ . First the value of  $v_i$  should be corrected for purely instrumental errors, either from a calibration curve for the indicator used or, better still, from a flight-history test.<sup>19</sup> The value of  $v_i$  as thus corrected is the one which should be used in the computation of  $\frac{Dv_i\rho}{\mu}$ . The value of  $\rho$  can be computed from equation 11 or can be obtained from Figure 19. The value of  $\mu$  can be obtained in C. G. S. units from equation (12), or from Table X. It should be remembered that  $D$  is assumed as 1 centimeter throughout this paper.

When using Figures 17a and 17b the values of  $v_i$ ,  $\rho$ , and  $\mu$  must be reduced to the centimeter-gram-second system. In case it is desired to utilize the correction curves in Figures 17a

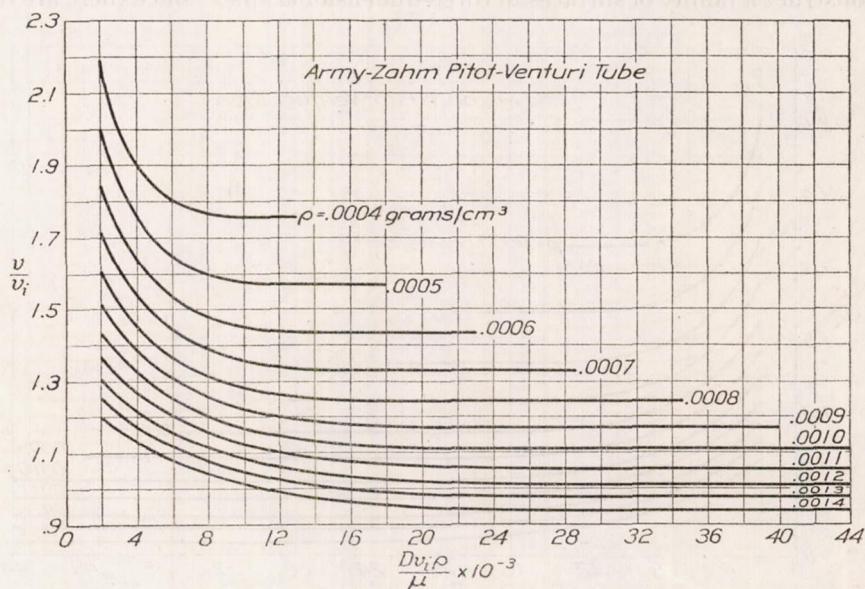


FIG. 17b.—Correction curves for the altitude effect.

and 17b using English units in place of metric, this can be accomplished by substituting in the variable  $\frac{Dv_i\rho}{\mu}$ ,  $D = 0.0328$  feet (the equivalent of 1 centimeter)  $v_i$  in feet per second,  $\rho$  in pounds per cubic foot, and  $\mu$  in pounds per foot per second.

Graphical methods can be developed easily for computing the values of  $\frac{Dv_i\rho}{\mu}$ , but will not be attempted in this paper.

#### 7. ILLUSTRATIVE EXAMPLES.

Two examples illustrating the use of the correction curves developed in this part of the report are given below. The first is based on the data obtained in the flight test referred to in Part I of Report 110, page 19. The determination of the true air speed is made by the methods which would be used in the office. The second example involves purely hypothetical data and illustrates the quick but approximate methods of reduction which could be used in the air.

##### EXAMPLE I.

The following data were obtained during a flight made at McCook Field on December 20, 1919, by one of the authors.

<sup>19</sup> A flight-history test is one in which the factors of time, barometric pressure, and instrument temperature are made to repeat in the laboratory the conditions of the flight.



Air speed from indicator using Army Zahm-type nozzle.....m.p.h.. 58  
 Altimeter reading.....feet.. 14,900  
 Air temperature.....°C.. -11  
 Indicated air speed  $v_i$  corrected from flight-history test<sup>20</sup>.....m.p.h.. 58.8  
 Altimeter reading, corrected from flight-history test,<sup>20</sup>.....feet.. 14,690  
 Barometric pressure corresponding to corrected altimeter reading (from Bureau of Standards altitude tables).....mm. mercury.. 443.6

$v_i = 58.8 \times 44.7 = 2,630$  centimeters per second.

$\rho = 0.000785$  gram per cubic centimeter, from Figure 19.

$\mu = 0.0001675$  gram per centimeter per second, from Table X.

$D = 1$  centimeter.

$$\frac{Dv_i\rho}{\mu} = \frac{2630 \times 0.000785}{0.0001675} = 12,320.$$

$\frac{v}{v_i} = 1.27$ , from Figure 17b.

$v = 1.27 \times 58.8 = 74.7$  m.p.h. true air speed.

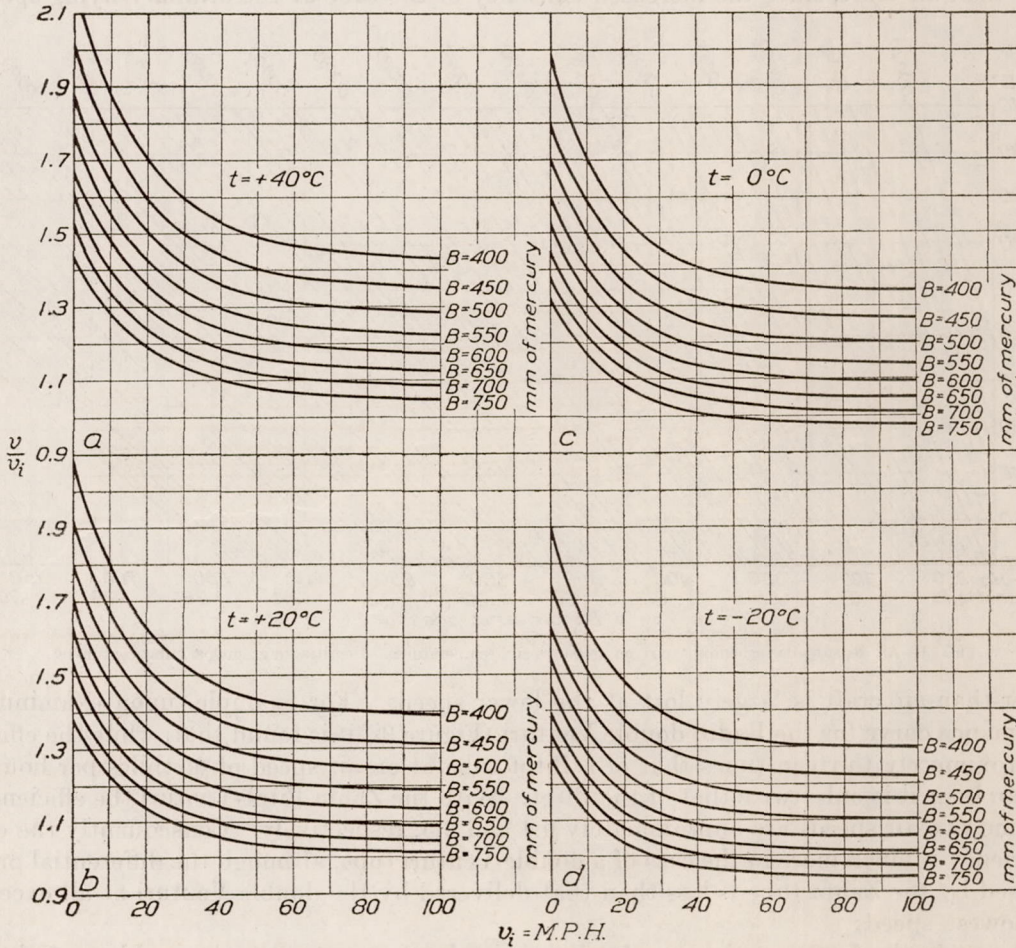


FIG. 18.—Correction curves for use in flight with Army and Navy Zahm Pitot-Venturi tubes.

EXAMPLE II.

The following observations were made on a dirigible airship during flight:

Indicated air speed (corrected for instrumental errors).....m.p.h.. 15  
 Altimeter reading.....feet.. 1,500  
 Air temperature.....°C.. +10  
 Barometric pressure corresponding to 1,500 feet altitude from Bureau of Standards altitude tables.....mm. mercury.. 719

$\frac{v}{v_i} = 1.20$ , from Figure 18.

$v = 1.20 \times 15 = 18$  m.p.h. true air speed.

<sup>20</sup> For definition of flight-history test see footnote 19.



For purposes of comparison, the computation will be made, correcting for air density alone:

$$\frac{v}{v_i} = 1.02, \text{ from Figure 15.}$$

$$v = 1.02 \times 15 = 15.3 \text{ m. p. h. air speed, corrected for density only.}$$

The error thus involved by ignoring the viscosity correction is seen to be 2.7 miles per hour, or 15 per cent of the true air speed.

#### 8. CONCLUSIONS.

From the results which have been reported in this paper, it is possible to draw certain general conclusions as to the measurement of air speed.

It is obvious that it is of little benefit to use a double Venturi for the low-speed flight of lighter-than-air craft, since the increased efficiency of the tube at the ordinary flying speeds of

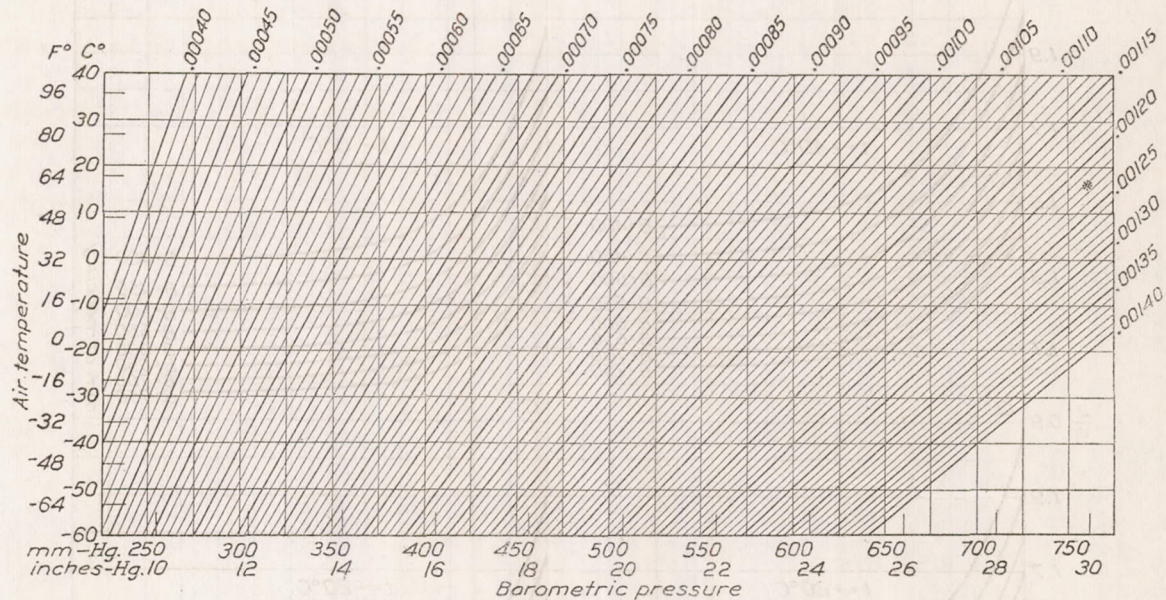


FIG. 19.—Air densities corresponding to given pressures and temperatures. Densities in grams per cubic centimeter.

heavier-than-air craft is largely lost at the lower speeds. For example, upon examining the performance curve for the Badin double Venturi (Figure 9i) it is found that, while the efficiency is approximately thirteen times that of a Pitot tube at an air speed of 65 miles per hour, at 5 miles an hour it is only twice that of the Pitot. With the Zahm Pitot-Venturi the efficiencies at the same two air speeds are approximately 6.4 and 2.5, respectively. Consequently the change of efficiency is much more in the case of a double Venturi tube, although the differential pressure delivered by the Zahm tube is less than that delivered by the double Venturi at all except the very lowest speeds.

Owing to the fact that the use of a Venturi tube does not solve the problem of obtaining sufficiently high differential pressures at low speeds to make practicable the construction of an indicator which will measure these pressures, it seems advisable to adopt a different type of indicator for such conditions. The cup or vane anemometer and the pressure plate are the two types which suggest themselves as suitable for low-speed measurements.

A cup anemometer air-speed indicator which is direct reading has been constructed at the Bureau of Standards and has met both laboratory and flight tests satisfactorily. This instrument when tested in the low-pressure wind tunnel at reduced pressures, showed less than 5 per cent altitude effect up to an altitude of 30,000 feet. Consequently the performance of this indicator is nearly independent of density. Furthermore, since the calibration curve of the



instrument was practically a straight line over its entire range (10 to 90 miles per hour), it has very nearly a uniform scale.

A pressure plate air-speed indicator might be designed to function accurately at low speeds, but it would certainly be subject to the density effect as expressed by equation (3a) and might be affected by viscosity or by some other change in the nature of the air flow at low speeds.

The Venturi or the Pitot-Venturi tube will continue to have advantages for use on heavier-than-air craft, since its construction and installation are simple and the differential pressure is so great that the indicators can be easily manufactured.

The correction curves, Figures 17a, 17b, and 18, given in this paper can be relied on for use with the Zahm tubes, provided the latter are not damaged.

The construction of similar correction curves for the Toussaint-Lepère tubes would not be justified, since these tubes are not subject to rigid construction specifications. While a set of curves representing the corrections for an average Toussaint-Lepère nozzle would probably give results which were more accurate than if the viscosity correction was entirely ignored, there would be so much uncertainty involved, owing to lack of information as to the calibration curve for the particular instrument, that the slight increase in accuracy hardly justifies the difficulty with which it is attained.

The authors wish to express their appreciation of the assistance of Mr. C. T. Buckingham and Mr. D. E. Merris of the Aeronautic Instruments Section of the Bureau of Standards in conducting the low-pressure wind-tunnel tests and in carrying out the laborious computations involved in this report. Mr. G. H. Keulegan also gave valuable assistance in determining the form of the unknown function.  $\theta \left( \frac{\rho_0}{\rho}, \frac{Dv_i \rho}{\mu} \right)$ .

TABLE IX.—U. S. Standard Air.

Altitude 1,000 feet.	Pressure (mm. Hg.).	Temperature (°C.).	Density (grams cm. <sup>3</sup> ).
0	760.0	15.0	0.001225
1	733.0	12.2	.001191
2	706.9	10.7	.001156
3	681.2	8.7	.001122
4	656.6	6.7	.001089
5	632.7	4.8	.001057
6	609.3	2.9	.001025
7	586.7	+ 1.1	.000993
8	564.9	- 0.6	.000963
9	543.8	- 2.3	.000932
10	523.2	- 3.9	.000903
11	503.4	- 5.5	.000873
12	484.4	- 7.0	.000845
13	465.8	- 8.5	.000817
14	447.8	-10.0	.000790
15	430.5	-11.3	.000764
16	414.0	-12.7	.000739
17	397.8	-14.0	.000713
18	382.3	-15.2	.000688
19	367.5	-16.4	.000665
20	353.1	-17.5	.000640
21	339.1	-18.7	.000619
22	325.6	-19.7	.000597
23	312.9	-20.8	.000576
24	300.5	-21.8	.000555
25	288.5	-22.7	.000535
26	277.1	-23.6	.000516
27	265.9	-24.5	.000497
28	255.3	-25.4	.000479
29	245.1	-26.2	.000461
30	235.2	-27.0	.000443



TABLE X.—*Air Viscosities by Sutherland's Formula.*

Temperature (°C.).	Values of air viscosity (gms./cm.sec.).	Temperature (°C.).	Values of air viscosity (gms./cm.sec.).
-40	0.0001520	+ 5	0.0001758
-35	.0001548	+10	.0001783
-30	.0001575	+15	.0001808
-25	.0001602	+20	.0001833
-20	.0001630	+25	.0001858
-15	.0001656	+30	.0001882
-10	.0001682	+35	.0001907
- 5	.0001708	+40	.0001930
0	.0001733		

## BIBLIOGRAPHY.

- "The Pitot Tube and other Anemometers for Aeroplanes," by W. H. Herschel, and the "Theory of the Pitot and Venturi Tubes," by E. Buckingham; Report No. 2 of the National Advisory Committee for Aeronautics, Pts. I and II, respectively, 1915.
- "Model Experiments and the Form of Empirical Equations," Transactions A. S. M. E., v. 36, pp. 263-296, 1915, by E. Buckingham.
- "Dimensional Theory of Wind Tunnel Experiments," Smithsonian Misc. Papers, v. 62-64, pp. 15-26, 1916, by E. Buckingham.
- "Development of Air Speed Nozzles" by A. F. Zahm; Report No. 31 of the National Advisory Committee for Aeronautics, 1918.
- "Ein Neues Instrument zur Geschwindigkeitsmessung auf Flugzeugen," W. Hort, Zeitschrift für Flugtechnik und Motorluftschiffahrt, vol. 9, 1918, p. 67.
- "The Altitude Effect on Air Speed Indicators," Pts. I and II, by M. D. Hersey, F. L. Hunt, and H. N. Eaton; Report No. 110 of the National Advisory Committee for Aeronautics, 1920.
- "Air Speed Indicators," by F. L. Hunt, and "Testing of Air Speed Indicators," by H. O. Stearns; Report No. 127 of the National Advisory Committee for Aeronautics, Pts. I and II, respectively.

---

ADDITIONAL COPIES  
OF THIS PUBLICATION MAY BE PROCURED FROM  
THE SUPERINTENDENT OF DOCUMENTS  
GOVERNMENT PRINTING OFFICE  
WASHINGTON, D. C.  
AT  
10 CENTS PER COPY

▽